HAL
open science

Stabilization and Best Actuator Location for the Navier–Stokes Equations

Christophe Airiau, Jean-Marie Buchot, Ritesh Kumar Dubey, Michel Fournié, Jean-Pierre Raymond, Jessie Weller

To cite this version:

Christophe Airiau, Jean-Marie Buchot, Ritesh Kumar Dubey, Michel Fournié, Jean-Pierre Raymond, et al.. Stabilization and Best Actuator Location for the Navier–Stokes Equations. SIAM Journal on Scientific Computing, 2017, 39 (5), pp.B993-B1020. 10.1137/16M107503X . hal-01810784

HAL Id: hal-01810784

https://hal.science/hal-01810784v1

Submitted on 8 Jun 2018

HAL is a multi-disciplinary open access archive for the deposit and dissemination of scientific research documents, whether they are published or not. The documents may come from teaching and research institutions in France or abroad, or from public or private research centers.

L'archive ouverte pluridisciplinaire **HAL**, est destinée au dépôt et à la diffusion de documents scientifiques de niveau recherche, publiés ou non, émanant des établissements d'enseignement et de recherche français ou étrangers, des laboratoires publics ou privés.

Open Archive TOULOUSE Archive Ouverte (OATAO)
OATAO is an open access repository that collects the work of Toulouse researchers and makes it freely available over the web where possible.

This is an author-deposited version published in : http://oatao.univ-toulouse.fr/
Eprints ID : 20145

To link to this article : DOI:10.1137/16M107503X
URL : https://doi.org/10.1137/16M107503X

To cite this version : Airiau, Christophe and Buchot, Jean-Marie and Dubey, Ritesh Kumar and Fournié, Michel and Raymond, Jean-Pierre and Weller, Jessie *Stabilization and Best Actuator Location for the Navier--Stokes Equations.* (2017) SIAM Journal on Scientific Computing, vol. 39 (n° 5). pp. B993-B1020. ISSN 1064-8275

Any correspondence concerning this service should be sent to the repository administrator: staff-oatao@listes-diff.inp-toulouse.fr

STABILIZATION AND BEST ACTUATOR LOCATION FOR THE NAVIER–STOKES EQUATIONS*

CHRISTOPHE AIRIAU†, JEAN-MARIE BUCHOT‡, RITESH KUMAR DUBEY§, MICHEL FOURNIÉ‡, JEAN-PIERRE RAYMOND‡, AND JESSIE WELLER-CALVO†

Abstract. We study the numerical approximation of the boundary stabilization of the Navier–Stokes equations with mixed Dirichlet/Neumann boundary conditions, around an unstable stationary solution in a two dimensional domain. We first derive a semidiscrete controlled system, coming from a finite element approximation of the Navier–Stokes equations, which is new in the literature. We propose a new strategy for finding a boundary feedback control law able to stabilize the nonlinear semidiscrete controlled system in the presence of boundary disturbances. We determine the best control location. Next, we study the degree of stabilizability of the different real generalized eigenspaces of the controlled system. Based on that analysis, we determine an invariant subspace $\mathbb{Z}_u$ and the projection of the controlled system onto $\mathbb{Z}_u$. The projected system is used to determine feedback control laws. Our numerical results show that this control strategy is quite efficient when applied to the Navier–Stokes system for a Reynolds number $R_e = 150$ with boundary perturbations.

Key words. Navier–Stokes equations, feedback boundary control, boundary perturbation, best actuator location

1. Introduction.

1.1. Setting of the problem. We study the numerical approximation of the boundary stabilization of the Navier–Stokes equations with mixed Dirichlet/Neumann boundary conditions, around an unstable stationary solution in a two dimensional domain. The system is subject to disturbances in an inflow boundary condition, and the control acts through a Dirichlet boundary condition. In the model that we consider, Ω is a bounded domain in $\mathbb{R}^2$ with boundary $\Gamma = \Gamma_d \cup \Gamma_n$, Γ_d (resp., Γ_n) is the part of Γ where Dirichlet (resp., Neumann) boundary conditions are prescribed. We assume that (w_s, q_s) is a real valued solution to the stationary Navier–Stokes equations

$$\begin{aligned} &(w_s \cdot \nabla) w_s - \operatorname{div} \sigma(w_s, q_s) = 0, \quad \operatorname{div} w_s = 0 \quad \text{in} \quad \Omega, \\ &w_s = u_s \quad \text{on} \quad \Gamma_d, \qquad \sigma(w_s, q_s) n = 0 \quad \text{on} \quad \Gamma_n, \end{aligned} \tag{1.1}$$

Funding: The third author was supported by the CEFIPRA Project 3701-1, Control of Systems of Partial Differential Equations. The sixth author was supported by the ANR-Project Cormored BLAN-0115. The first, second, and fifth authors were partially supported by the FNRAE foundation under the project ECOSEA.

†IMFT, UMR CNRS/INPT/UPS 5502, Toulouse University, Toulouse 31400, France (christophe.airiau@imft.fr, jessie.wellercalvo@gmail.com).

‡IMT, UMR 5219, Université Paul Sabatier Toulouse III & CNRS, 31062 Toulouse Cedex, France (jean-marie.buchot@math.univ-toulouse.fr, michel.fournie@math.univ-toulouse.fr, raymond@math.univ-toulouse.fr).

§Research Institute, SRM University, Kattankulathur 603203, Kancheepuran, Tamilnadu, India (riteshkd@gmail.com).

where $\sigma(w_s, q_s) = \nu(\nabla w_s + (\nabla w_s)^T) - q_s I$ is the Cauchy stress tensor and $\nu > 0$ is the kinematic viscosity of the fluid. We consider the case where (w_s, q_s) is an unstable solution of the following system:

$$
\begin{aligned}
&\frac{\partial w}{\partial t} + (w \cdot \nabla) w - \operatorname{div} \sigma(w, q) = 0, \quad \operatorname{div} w = 0 \quad \text{in} \quad Q_\infty = \Omega \times (0, \infty), \\
&w = u_s + v_c + v_d \quad \text{on} \quad \Sigma_d^\infty, \qquad \sigma(w, q) n = 0 \quad \text{on} \quad \Sigma_n^\infty, \\
&w(0) = w_s + z_0 \quad \text{on} \quad \Omega,
\end{aligned} \tag{1.2}
$$

with $\Sigma_d^\infty = \Gamma_d \times (0, \infty)$ and $\Sigma_n^\infty = \Gamma_n \times (0, \infty)$. In this setting w denotes the fluid velocity, q is the fluid pressure, z_0 is a perturbation of the stationary velocity w_s, v_c is the control function with support in $\Gamma_c \times (0, \infty) \subset \Sigma_d^\infty$, u_s is supported in $\Gamma_i \subset \Gamma_d$, and v_d is a time dependent disturbance, with support in $\Gamma_i \times (0, \infty)$. It plays the role of an unknown model error in the inflow boundary condition, and we assume that it is of the form $v_d(x, t) = \mu(t)\, h(x)$. We choose v_c of the form

$$
v_c(x, t) = \sum_{i=1}^{N_c} v_i(t)\, g_i(x). \tag{1.3}
$$

The functions g_i are the supports of the actuators; their location can be chosen in the control zone Γ_c to improve the efficiency of the control. We shall explain later on how we can determine the *best control location*. The function $v = (v_i)_{1 \le i \le N_c}$ is the control variable.

As noticed in [26], if $(v_c(\cdot, 0), v_d(\cdot, 0)) \neq (0, 0)$, the initial condition $w(0) = w_s + z_0$ has to be replaced by $\Pi w(0) = \Pi(w_s + z_0)$, where Π is the Leray projector defined in section 2.2. Setting $z = w - w_s$ and $p = q - q_s$, the nonlinear system satisfied by (z, p) is

$$
\begin{aligned}
&\frac{\partial z}{\partial t} + (w_s \cdot \nabla) z + (z \cdot \nabla) w_s + (z \cdot \nabla) z - \operatorname{div} \sigma(z, p) = 0, \quad \operatorname{div} z = 0 \text{ in } Q_\infty, \\
&z = v_c + v_d \quad \text{on} \quad \Sigma_d^\infty, \quad \sigma(z, p) n = 0 \text{ on } \Sigma_n^\infty, \quad \Pi z(0) = \Pi z_0 \text{ in } \Omega,
\end{aligned} \tag{1.4}
$$

while the linearized system is

$$
\begin{aligned}
&\frac{\partial z}{\partial t} + (w_s \cdot \nabla) z + (z \cdot \nabla) w_s - \operatorname{div} \sigma(z, p) = 0, \quad \operatorname{div} z = 0 \quad \text{in} \quad Q_\infty, \\
&z = v_c + v_d \text{ on } \Sigma_d^\infty, \quad \sigma(z, p) n = 0 \text{ on } \Sigma_n^\infty, \quad \Pi z(0) = \Pi z_0 \quad \text{in } \Omega.
\end{aligned} \tag{1.5}
$$

Let us emphasize that all the data and the solutions to the above equations are real valued. As is well known, contrary to the stationary Navier–Stokes equation with nonhomogeneous Dirichlet boundary conditions, in the case of mixed or Neumann boundary conditions, the existence of a weak solution to (1.1) is guaranteed only under smallness conditions on the datum u_s (see, e.g., [23] or [16]). The existence of solution (w_s, q_s) when u_s is a parabolic profile and when the channel in Figure 2.1 is long enough is analyzed in [26, appendix].

1.2. Semidiscrete approximations and control strategy. The stabilization of system (1.4) by a control of finite dimension in feedback form has been recently studied in [26]. When we approximate systems (1.4) and (1.5) by a finite element method, the nonhomogeneous Dirichlet boundary conditions can be taken into account either in strong form by imposing the value of the fluid flow at the boundary, or in weak form by adding a Lagrange multiplier. Despite its importance for the control of fluid

flows, the representation of semidiscrete approximations as controlled systems with a control acting on the boundary has not been extensively studied in the literature.

In the case of mixed boundary conditions, the representation of the incompressible Navier–Stokes equations as a controlled system is quite recent; see [26]. Obtaining similar results for the corresponding semidiscrete models is a crucial step to next develop a numerical control strategy. Indeed, a very good numerical algorithm for model reduction or for solving large scale Riccati equations will not be efficient if the representation of the underlying discrete model, in the form of a controlled system, is not accurate enough.

For the infinite dimensional model corresponding to the Navier–Stokes equations or the linearized Navier–Stokes equations, the weak and strong formulations for Dirichlet boundary conditions lead to the same controlled systems. This is no longer true for semidiscrete models.

For stationary Navier–Stokes equations the numerical treatment of nonhomogeneous Dirichlet boundary conditions either in strong form or in weak form is well studied in the literature; see [17].

The representation as controlled systems of semidiscrete approximations of the Navier–Stokes equations is usually done by using the so-called Leray or Helmholtz projector. In the case of nonhomogeneous Dirichlet boundary conditions, with a nonzero normal component, the Leray projection of the velocity is different from the velocity. Because of that, the state variable of the controlled system is not the velocity but its projection. An additional equation has to be added for the remaining part of the velocity. This decomposition is an essential step to stabilize the Navier–Stokes system by a feedback boundary control (see [26, 29, 30, 31]).

In this paper, we take into account the nonhomogeneous Dirichlet boundary conditions in a weak form, by introducing an additional Lagrange multiplier $\boldsymbol{\tau}(t)$. It is convenient to concatenate the two Lagrange multipliers $\mathbf{p}(t)$ (the discrete approximation of the pressure) and $\boldsymbol{\tau}(t)$, and to introduce the vector $\boldsymbol{\eta} = (\eta_1, \cdots, \eta_{N_\eta})^T = (p_1, \cdots, p_{N_p}, \tau_1, \cdots, \tau_{N_\tau})^T$. The semidiscrete model is of the form

(1.6)
$$M_{zz}\mathbf{z}'(t) = A_{zz}\mathbf{z}(t) + A_{z\eta}\boldsymbol{\eta}(t), \quad \mathbb{\Pi}^T\mathbf{z}(0) = \mathbb{\Pi}^T\mathbf{z}_0, \quad A_{z\eta}^T\mathbf{z}(t) - M_{\eta\eta}\,\mathbf{G}\,\mathbf{v}(t) = 0,$$

where $\mathbb{\Pi}$ is the discrete Leray projector of the system and $\mathbf{G}$ is the matrix whose columns are the coordinate vectors of the actuators g_i. The mass matrices are $M_{zz} \in \mathbb{R}^{N_z \times N_z}$ and $M_{\eta\eta} \in \mathbb{R}^{N_\eta \times N_\eta}$, and the stiffness matrices are $A_{zz} \in \mathbb{R}^{N_z \times N_z}$ and $A_{z\eta} \in \mathbb{R}^{N_z \times N_\eta}$. We assume that $N_\eta < N_z$ and that $A_{z\eta}$ is of rank N_η. We prove that $(\mathbf{z}, \boldsymbol{\eta})$ is the solution of (1.6) if and only if it is the solution to

$$\begin{aligned}
&\mathbb{\Pi}^T\mathbf{z}'(t) = \mathbf{A}\,\mathbb{\Pi}^T\mathbf{z}(t) + \mathbf{B}\mathbf{v}(t), \quad \mathbb{\Pi}^T\mathbf{z}(0) = \mathbb{\Pi}^T\mathbf{z}_0,\\
&(I - \mathbb{\Pi}^T)\mathbf{z}(t) = M_{zz}^{-1}A_{z\eta}(A_{z\eta}^T M_{zz}^{-1}A_{z\eta})^{-1}M_{\eta\eta}\,\mathbf{G}\,\mathbf{v}(t),\\
&\boldsymbol{\eta}(t) = (A_{z\eta}^T M_{zz}^{-1}A_{z\eta})^{-1}A_{z\eta}^T\mathbf{z}'(t) - (A_{z\eta}^T M_{zz}^{-1}A_{z\eta})^{-1}A_{z\eta}^T M_{zz}^{-1}A_{zz}\mathbf{z}(t),
\end{aligned} \tag{1.7}$$

where the matrix $\mathbf{A}$ and the control operator $\mathbf{B}$ are defined by

$$\mathbf{A} = \mathbb{\Pi}^T M_{zz}^{-1}A_{zz} \quad \text{and} \quad \mathbf{B} = \mathbf{A}M_{zz}^{-1}A_{z\eta}(A_{z\eta}^T M_{zz}^{-1}A_{z\eta})^{-1}M_{\eta\eta}\,\mathbf{G}.$$

Thus, we have determined the pair $(\mathbf{A}, \mathbf{B})$ needed for any control strategy of the linearized system (1.6) or, equivalently, (1.7). We prove that the family $(g_i)_{1\le i\le N_c}$ can be chosen so that the pair $(\mathbf{A}, \mathbf{B})$ is stabilizable in $\mathrm{Ker}(A_{z\eta}^T)$ (see Proposition 2.1 for the stabilizability of the infinite dimensional model and Remark 3.10 for the stabilizability of the semidiscrete model).

Due to the definition of $\mathbb{\Pi}^T$, we have $\mathbb{R}^{N_z} = \mathrm{Ker}(A_{z\eta}^T) \oplus \mathrm{Ker}(\mathbf{A}\mathbb{\Pi}^T)$, and $\mathrm{Ker}(A_{z\eta}^T) = \oplus_{\boldsymbol{\lambda}_j \neq 0, \mathrm{Im}\boldsymbol{\lambda}_j \geq 0} G_{\mathbb{R}}(\boldsymbol{\lambda}_j)$, where $G_{\mathbb{R}}(\boldsymbol{\lambda}_j)$ is the real generalized eigenspace associated with $\boldsymbol{\lambda}_j \in \mathrm{spect}(\mathbf{A}\mathbb{\Pi}^T)$. We choose a family $(\boldsymbol{\lambda}_j)_{j \in J_u}$ containing all the unstable eigenvalues (with nonnegative imaginary part) of $\mathbf{A}\mathbb{\Pi}^T$ and eventually the most stabilizable eigenmodes (with nonnegative imaginary part), and we set $\mathbb{Z}_u = \oplus_{j \in J_u} G_{\mathbb{R}}(\boldsymbol{\lambda}_j)$. Thus, we have a decomposition of $\mathrm{Ker} A_{z\eta}^T$ of the form

$$\mathrm{Ker}(A_{z\eta}^T) = \mathbb{Z}_u \oplus \mathbb{Z}_s \quad \text{with} \quad \mathbf{A}\mathbb{Z}_u \subset \mathbb{Z}_u \quad \text{and} \quad \mathbf{A}\mathbb{Z}_s \subset \mathbb{Z}_s, \tag{1.8}$$

and $\mathbf{A}|_{\mathbb{Z}_s}$ is exponentially stable. To stabilize system (1.6), it is enough to stabilize the system obtained by projecting system (1.6) onto $\mathbb{Z}_u$ parallel to $\mathbb{Z}_s$.

Our control strategy is based on a hierarchical procedure consisting in the following steps:

1. After deriving the semidiscrete controlled system, we first determine the best control location. Next, we study the degree of stabilizability of the different real generalized eigenspaces of the semidiscrete controlled system. Based on that analysis, we determine an invariant subspace $\mathbb{Z}_u$ used to define a reduced order model.

2. We next choose some parameters, in the Riccati equation used to calculate feedback control laws, to stabilize efficiently the transient regime of the closed-loop linearized system. That is essential when the feedback law is used to stabilize the nonlinear system. There is a compromise to be found between the efficiency of the control law and the amplitude of the control.

3. We compare the efficiency of different feedback laws for the nonlinear system with boundary perturbations, by varying the choice of $\mathbb{Z}_u$ and of the Riccati equations used to determine the feedback gains.

Even if it is not detailed for reasons of length, our approach allows us to show that the feedback control laws for the semidiscrete controlled system are finite element approximations of feedback control laws of the infinite dimensional controlled system.

Let us finally make some comparisons with related papers in the literature.

In [19] the authors deal with model reductions for stable linearized Navier–Stokes equations. The semidiscretization of the PDE system is performed with a P_2–P_1 finite element method and a strong formulation for the nonhomogeneous Dirichlet boundary control. As noticed in section 8, in this approach the time derivative of the control appears in the semidiscrete algebraic differential system. For stable systems as in [19], the time derivative of the control may be removed when a mass lumping method is used (see section 8 and [12]). With this choice, the algebraic differential system in [19, eqs. (1.1a), (1.1b)] is of the same type as system (1.6). But obviously the unknowns are different. Thus, even if the controlled system [19, eqs. (6.6a), (6.6b)] looks very similar to our controlled system (1.7), the variables of the two systems do not have the same meaning and do not play the same role.

In [6], a lifting procedure is also used to treat the boundary controls. But unlike the approach in [19], the time derivative of the control, appearing via this lifting, is not removed, and it is taken into account in an extended system. See also [8] for numerical tests comparing different ways of dealing with nonhomogeneous boundary conditions for convection diffusion equations.

In the two papers [9] and [5], a lifting procedure is also used to deal with Dirichlet controls in a strong form. As in [19], the time derivative of the control is dropped out, which simplifies the derivation of the controlled system (see section 8), but which, according to our experience in [12], may affect the numerical accuracy for unstable systems. The lifting procedure in [5, section 2.4] is different from the one in [19].

It uses a Leray projector. However, the Leray projector introduced [5, page A837], together with the decomposition of L^2 vector fields, is not consistent with the mixed boundary conditions considered in those papers (compare with (2.1)).

In [10], the authors study the reduction of the shedding of vortices behind a circular cylinder by rotation. We can notice that even if the shedding of vortices is reduced, the stabilization is far from being achieved. In the case of a distributed control, the approach based on the projection onto an unstable subspace has been used in [1]. See also the review paper [14] about control strategies of wakes behind a bluff body.

The plan of the current paper is as follows. Throughout section 2 we recall results from [26] that are used in the paper. In section 3, we describe the finite element approximation of system (1.5). The projected dynamical system of small dimension, needed to determine feedback control laws, is derived in section 3.5. We explain in section 3.6 how we can determine feedback control laws stabilizing the nonlinear semidiscrete system. Section 4 is dedicated to the numerical approximation of the linearized Navier–Stokes system and to the determination of the associated spectrum. In section 5, we introduce criteria used for finding the best control location and the degree of stabilizability. The stabilization results for the Navier–Stokes equations are reported in section 6. Finally, in an appendix (section 8), we treat the case of Dirichlet boundary conditions without Lagrange multiplier, and we clearly see that the approach with Lagrange multiplier leads to a much simpler system.

2. The infinite dimensional model.

2.1. The geometrical configuration. Let us now describe more precisely the problem we deal in the numerical tests. The geometrical domain corresponds to a flow around a circular cylinder in a rectangular channel; see Figure 2.1. The dimensions of the domain are $\Omega = (-1.5, 2.2) \times (0, 0.4) \setminus \text{Disc}$, where "Disc" is the disc centered at $(0.25, 0.2)$ with radius $r_c = 0.05$. The boundary of the disc is denoted by Γ_c. The inflow boundary is $\Gamma_i = \{-1.5\} \times [0, 0.4]$, the outflow boundary is $\Gamma_n = \{2.2\} \times [0, 0.4]$, and homogeneous boundary conditions are prescribed on $\Gamma_0 = (-1.5, 2.2) \times \{0\} \cup (-1.5, 2.2) \times \{0.4\}$. For more general configurations to which the present results of the paper may be applied, we refer the reader to [26].

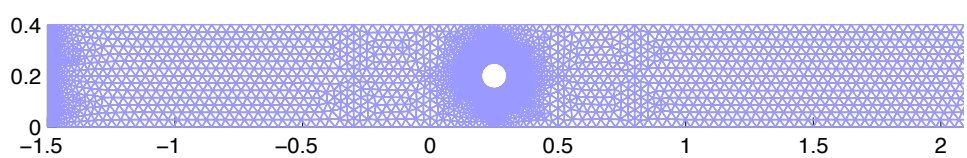

FIG. 2.1. *Geometrical configuration and triangular mesh used for simulations.*

2.2. The Oseen operator. In the case of mixed Dirichlet/Neumann boundary conditions, we introduce the space

$$V^0_{n,\Gamma_d}(\Omega) = \Big\{ z \in L^2(\Omega; \mathbb{R}^2) \mid \operatorname{div} z = 0 \text{ in } \Omega,\ z \cdot n = 0 \text{ on } \Gamma_d \Big\}.$$

We have the following orthogonal decomposition:

$$L^2(\Omega; \mathbb{R}^2) = V^0_{n,\Gamma_d}(\Omega) \oplus \operatorname{grad} H^1_{\Gamma_n}(\Omega), \quad H^1_{\Gamma_n}(\Omega) = \{ p \in H^1(\Omega) \mid p = 0 \text{ on } \Gamma_n \}.$$

The Leray projector Π is the orthogonal projector in $L^2(\Omega;\mathbb{R}^2)$ onto $V^0_{n,\Gamma_d}(\Omega)$. It can be easily shown that $\Pi z = z - \nabla p_z - \nabla q_z$ for every $z \in L^2(\Omega;\mathbb{R}^2)$, where p_z and q_z satisfy

$$\begin{aligned} &p_z \in H^1_0(\Omega), \quad \Delta p_z = \operatorname{div} z \in H^{-1}(\Omega), \\ &q_z \in H^1_{\Gamma_n}(\Omega), \quad \Delta q_z = 0, \quad \frac{\partial q_z}{\partial n} = (z - \nabla p_z)\cdot n \quad \text{on } \Gamma_d, \quad q_z = 0 \quad \text{on } \Gamma_n. \end{aligned} \tag{2.1}$$

To define the Oseen operator, we introduce the spaces

$$H^1_{\Gamma_d}(\Omega;\mathbb{R}^2) = \{z \in H^1(\Omega;\mathbb{R}^2) \mid z = 0 \text{ on } \Gamma_d\} \quad \text{and} \quad V^1_{\Gamma_d}(\Omega) = H^1_{\Gamma_d}(\Omega;\mathbb{R}^2) \cap V^0_{n,\Gamma_d}(\Omega).$$

The Stokes operator A_0 is defined by $A_0 z = \Pi \operatorname{div} \sigma(z,p)$ for functions $z \in V^1_{\Gamma_d}(\Omega) \cap H^{3/2+\varepsilon_0}(\Omega;\mathbb{R}^2)$ with $\varepsilon_0 > 0$, for which there is a pressure $p \in H^{1/2+\varepsilon_0}(\Omega)$ such that $\operatorname{div}\sigma(z,p) \in L^2(\Omega;\mathbb{R}^2)$ and $\sigma(z,p)n = 0$ on Γ_n; see [26, Theorem 2.10]. The Oseen operator $(A, \mathcal{D}(A))$ is defined by $\mathcal{D}(A) = \mathcal{D}(A_0)$ and $Az = A_0 z + \Pi\big((w_s\cdot\nabla)z + (z\cdot\nabla)w_s\big)$. The adjoint operator of $(A,\mathcal{D}(A))$ is defined in [26, Theorem 2.11].

2.3. The controlled system. We define the lifting operator $L \in \mathcal{L}(L^2(\Gamma_c;\mathbb{R}^2), L^2(\Omega;\mathbb{R}^2))$ by setting $Lg = \xi$ for all $g \in L^2(\Gamma_c;\mathbb{R}^2)$, where (ξ,ψ) is the solution to the stationary equation

$$\begin{aligned} &\lambda_0 \xi - \operatorname{div}\sigma(\xi,\psi) + (w_s\cdot\nabla)\xi + (\xi\cdot\nabla)w_s = 0, \quad \operatorname{div}\xi = 0 \quad \text{in} \quad \Omega, \\ &\xi = g \quad \text{on } \Gamma_d, \quad \sigma(\xi,\psi)n = 0 \quad \text{on} \quad \Gamma_n, \end{aligned}$$

for some $\lambda_0 > 0$ belonging to the resolvent set of A. In [26], we have shown that if $v \in H^1_0(0,\infty;\mathbb{R}^{N_c})$ and $z_0 \in V^1_{\Gamma_d}(\Omega)$, a function $z \in L^2_{\text{loc}}([0,\infty);H^1(\Omega;\mathbb{R}^2))$ is a solution to (1.5) in the sense of transposition if and only if $(\Pi z, (I-\Pi)z)$ is the solution to the system

$$\begin{aligned} &\Pi z' = A\Pi z + \textstyle\sum_{i=1}^{N_c} v_i D_A g_i = A\Pi z + Bv, \qquad \Pi z(0) = z_0, \\ &(I-\Pi)z = (I-\Pi)\left(\textstyle\sum_{i=1}^{N_c} v_i(\tau)\, Lg_i\right), \end{aligned} \tag{2.2}$$

with $D_A = (\lambda_0 I - A)\Pi L \in \mathcal{L}(L^2(\Gamma_d;\mathbb{R}^2), (\mathcal{D}(A^*))')$.

2.4. Projected systems. The spectrum of A, denoted by $\operatorname{spect}(A)$, is contained in a sector of the form $\{\lambda \in \mathbb{C} \mid \lambda - \omega_0 = re^{\pm i\vartheta},\ r > 0,\ \vartheta > \vartheta_0\}$ with $\vartheta_0 > \frac{\pi}{2}$. The eigenvalues of A, denoted by $(\lambda_j)_{j\in\mathbb{N}^*}$, are isolated and of finite multiplicity (see [26]). Since w_s is real valued, they are either real or pairwise conjugate when they are not real. We denote by $G_{\mathbb{R}}(\lambda_j)$ the real generalized eigenspace for A associated with λ_j, that is, the space generated by $\operatorname{Re} G_{\mathbb{C}}(\lambda_j) \cup \operatorname{Im} G_{\mathbb{C}}(\lambda_j)$ (where $G_{\mathbb{C}}(\lambda_j)$ is the complex generalized eigenspace for A), and by $G^*_{\mathbb{R}}(\lambda_j)$ the real generalized eigenspace for A^*. We set

$$Z_u = \oplus_{j\in J_u} G_{\mathbb{R}}(\lambda_j) = \operatorname{vect}\{e_1,\cdots,e_{d_u}\}, \quad Z^*_u = \oplus_{j\in J_u} G^*_{\mathbb{R}}(\lambda_j) = \operatorname{vect}\{\xi_1,\cdots,\xi_{d_u}\},$$

where J_u is a finite subset of $\mathbb{N}$ such that the family $(\lambda_j)_{j\in J_u}$ contains all the unstable eigenmodes of A, d_u is the dimension of Z_u, and we assume that the two bases $\{e_1,\cdots,e_{d_u}\}$ and $\{\xi_1,\cdots,\xi_{d_u}\}$ satisfy the following biorthogonality condition:

$$(e_i,\xi_k)_{L^2(\Omega;\mathbb{R}^2)} = \delta_{ik} \quad \text{for all } 1 \le i \le d_u \text{ and all } 1 \le k \le d_u.$$

We denote by Z_s the invariant subspace of A and by Z_s^* the invariant subspace of A^* such that

$$V^0_{n,\Gamma_d}(\Omega) = Z_u \oplus Z_s \quad \text{and} \quad V^0_{n,\Gamma_d}(\Omega) = Z_u^* \oplus Z_s^*.$$

We have that $\mathrm{Respect}(A|_{Z_s}) < -\alpha_s \leq 0$, because the unstable subspace of A is included in Z_u. We set $A_u = A|_{Z_u}$, $A_s = A|_{Z_s}$, $A_u^* = A^*|_{Z_u^*}$, $A_s^* = A^*|_{Z_s^*}$. Thus we have

$$\|e^{tA_s}\|_{\mathcal{L}(V^0_{n,\Gamma_d}(\Omega))} \leq C\, e^{-\alpha_s t} \quad \text{and} \quad \|e^{tA_s^*}\|_{\mathcal{L}(V^0_{n,\Gamma_d}(\Omega))} \leq C\, e^{-\alpha_s t} \quad \text{for all } t > 0.$$

2.5. Stabilizability issues for the pair (A, B). For each $j \in J_u$, we denote by $(\phi_j^k)_{1\leq k\leq \ell_j}$ a basis of the complex vector space $\mathrm{Ker}(A^* - \lambda_j I)$ (thus $\ell_j = \dim(\mathrm{Ker}(A^* - \lambda_j I))$), and by $(\psi_j^k)_{1\leq k\leq \ell_j}$ the family of associated pressures. Since A is not self-adjoint, the eigenvalues λ_j may be complex (there are pairs of complex conjugate eigenvalues), and the eigenfunctions ϕ_j^k may have complex values. Now we choose $\omega > 0$ such that $\mathrm{Respect}(A|_{Z_u}) > -\omega$, and we set $A_{\omega,u} = \pi_u(A + \omega I)$ and $B_u = \pi_u B$, where π_u is the projection on Z_u parallel to Z_s. From [4, Theorem 3], it follows that $(A_{\omega,u}, B_u)$ is stabilizable if and only if

$$\text{for all } j \in J_u, \text{ the family} \qquad \left(\int_{\Gamma_c} \sigma(\phi_j^k, \psi_j^k) n \cdot g_1, \cdots, \int_{\Gamma_c} \sigma(\phi_j^k, \psi_j^k) n \cdot g_{N_c}\right)_{1\leq k\leq \ell_j} \text{ is of rank } \ell_j. \tag{2.3}$$

PROPOSITION 2.1 (see [26, Theorem 3.2]). *Let m be a function of class C^2 defined on Γ_c with values in $[0,1]$, and equal to 1 on a nonempty relatively open subset of Γ_c. Let us choose the family $(g_i)_{1\leq i\leq N_c}$ such that it is a basis of the vector space*

$$\mathrm{vect}\{m\, \sigma(\xi_i, p_{\xi_i}) n \mid 1 \leq i \leq d_u\},$$

where $(\xi_i)_{1\leq i\leq d_u}$ is the basis of $\oplus_{j\in J_u} G^*_{\mathbb{R}}(\lambda_j)$ introduced above and $(p_{\xi_i})_{1\leq i\leq d_u}$ is the family of associated pressures. Then the family $(g_i)_{1\leq i\leq N_c}$ obeys condition (2.3).

According to that proposition it is always possible to find a family of functions $(g_i)_{1\leq i\leq N_c}$, with compact supports in Γ_c, satisfying (2.3). We now assume that $(g_i)_{1\leq i\leq N_c}$ obeys condition (2.3).

Remark 2.2. For the numerical simulations, we choose $N_c = 2$, and the functions $(g_i)_{1\leq i\leq 2}$ are defined in (4.2). The stabilizability of the semidiscrete system associated with the pair $(A_{\omega,u}, B_u)$ is tested numerically in section 5.2.

3. Semidiscrete systems.

3.1. Finite element approximation of system (1.5). To approximate system (1.5) by a finite element method, we introduce finite dimensional subspaces $X_h \subset H^1(\Omega; \mathbb{R}^2)$ for the velocity, $M_h \subset L^2(\Omega)$ for the pressure, and $S_h \subset L^2(\Gamma_d; \mathbb{R}^2)$ for the multipliers. We denote by $(\phi_i)_{1\leq i\leq N_z}$ a basis of X_h, by $(\psi_i)_{1\leq i\leq N_p}$ a basis of M_h, and by $(\zeta_i)_{1\leq i\leq N_\tau}$ a basis of S_h. Setting

$$z = \sum_{i=1}^{N_z} z_i \phi_i, \quad p = \sum_{i=1}^{N_p} p_i \psi_i, \quad \tau = \sum_{i=1}^{N_\tau} \tau_i \zeta_i, \quad z_0 = \sum_{i=1}^{N_z} z_{0,i} \phi_i, \quad g_i = \sum_{k=1}^{N_\tau} g_k^i \zeta_k,$$

if we denote by boldface letters the coordinate vectors, we have

$$\mathbf{z} = (z_1, \cdots, z_{N_z})^T, \quad \mathbf{p} = (p_1, \cdots, p_{N_p})^T, \quad \boldsymbol{\tau} = (\tau_1, \cdots, \tau_{N_\tau})^T,$$
$$\boldsymbol{\eta} = (p_1, \cdots, p_{N_p}, \tau_1, \cdots, \tau_{N_\tau})^T, \quad \mathbf{v} = (v_1, \cdots, v_{N_c})^T, \quad \mathbf{z}_0 = (z_{0,1}, \cdots, z_{0,N_z})^T.$$

When $v_d = 0$, the finite dimensional approximation of system (1.5) is the following:
(3.1)

Find $z \in H^1_{\rm loc}([0,\infty); X_h)$, $p \in L^2_{\rm loc}([0,\infty); M_h)$, $\tau \in L^2_{\rm loc}([0,\infty); S_h)$ such that

$$\frac{d}{dt}\int_\Omega z(t)\phi\,dx = a(z(t),\phi) + b(\phi,p(t)) + \langle \tau(t),\phi\rangle_{\Gamma_c} \quad \text{for all } \phi \in X_h,$$

$$b(z(t),\psi) = 0 \quad \text{for all } \psi \in M_h, \qquad \langle \zeta, z(t)\rangle_{\Gamma_d} = \textstyle\sum_{i=1}^{N_c} v_i(t)\langle \zeta, g_i\rangle_{\Gamma_c} \quad \text{for all } \zeta \in S_h,$$

where
(3.2)

$$a(z,\phi) = -\int_\Omega \Big(\frac{\nu}{2}(\nabla z + (\nabla z)^T) : (\nabla\phi + (\nabla\phi)^T) + ((w_s\cdot\nabla)z + (z\cdot\nabla)w_s)\phi\Big)\,dx,$$

$$b(\phi,p) = \int_\Omega {\rm div}\phi\, p\,dx \quad \text{and} \quad \langle \zeta, g_i\rangle_{\Gamma_c} = \int_{\Gamma_c} \zeta\, g_i\,dx.$$

In (3.1), we have assumed that $v_d = 0$. If $v_d(x,t) = \mu(t)\,h(x)$, the last equation in (3.1) reads as

$$\langle \zeta, z(t)\rangle_{\Gamma_d} = \sum_{i=1}^{N_c} v_i(t)\langle \zeta, g_i\rangle_{\Gamma_c} + \mu(t)\langle \zeta, h\rangle_{\Gamma_i} \quad \text{for all } \zeta \in S_h, \tag{3.3}$$

because the functions g_i are with support in Γ_c and h is with support in Γ_i. We do not specify the initial condition of system (3.1) because we are going to see that the natural initial condition $\mathbf{z}(0) = \mathbf{z}_0$ is not consistent with (3.1).

We introduce the stiffness matrices A_{zz}, A_{zp}, $A_{z\tau}$, $A_{z\eta}$; the mass matrices M_{zz}, $M_{\tau\tau}$, $M_{\eta\eta}$; and the matrix $\mathbf{G}$, the coefficients of which are defined by

$$A^{ij}_{zz} = a(\phi_j,\phi_i), \quad A^{ik}_{zp} = b(\phi_i,\psi_k) \quad \text{for } 1 \le i,\, j \le N_z,\ 1 \le k \le N_p,$$

$$A^{ij}_{z\tau} = \langle \zeta_j, \phi_i\rangle_{\Gamma_c} \quad \text{for } 1 \le i \le N_z,\ 1 \le j \le N_\tau, \quad A_{z\eta} = \begin{bmatrix} A_{zp} & A_{z\tau}\end{bmatrix},$$

$$M^{ij}_{zz} = (\phi_i,\phi_j), \quad 1 \le i,\, j \le N_z, \quad M^{k\ell}_{\tau\tau} = \langle \zeta_k, \zeta_\ell\rangle_{\Gamma_c}, \quad 1 \le k,\, \ell \le N_\tau,$$

$$M_{\eta\eta} = \begin{bmatrix} 0 \\ M_{\tau\tau}\end{bmatrix} \in \mathbb{R}^{N_\eta\times N_\tau}, \quad \text{and} \quad \mathbf{G} = [\mathbf{g}^1,\cdots,\mathbf{g}^{N_c}] = \begin{bmatrix} g^1_1 & \cdots & g^{N_c}_1 \\ \vdots & \vdots & \vdots \\ g^1_{N_\tau} & \cdots & g^{N_c}_{N_\tau}\end{bmatrix}.$$

We recall that $N_\eta = N_p + N_\tau < N_z$ and that $A_{z\eta}$ is of rank N_η. We also set

$$A = \begin{bmatrix} A_{zz} & A_{z\eta} \\ A^T_{z\eta} & 0\end{bmatrix} \quad \text{and} \quad M = \begin{bmatrix} M_{zz} & 0 \\ 0 & 0\end{bmatrix} \in \mathbb{R}^{(N_z+N_\eta)\times(N_z+N_\eta)}. \tag{3.4}$$

System (3.1) may be written in the form

$$M_{zz}\mathbf{z}'(t) = A_{zz}\mathbf{z}(t) + A_{z\eta}\boldsymbol{\eta}(t), \qquad 0 = A^T_{z\eta}\mathbf{z}(t) - M_{\eta\eta}\,\mathbf{G}\,\mathbf{v}(t). \tag{3.5}$$

3.2. Finite dimensional controlled system. In order to correctly define the initial condition for system (3.5) and to write it as a controlled system, we have to introduce the oblique projector in $\mathbb{R}^{N_z}$ onto ${\rm Ker}(A^T_{z\eta})$ parallel to ${\rm Im}(M^{-1}_{zz}A_{z\eta})$.

PROPOSITION 3.1. *The projector* $\mathbb{\Pi}$ *in* $\mathbb{R}^{N_z}$ *onto* ${\rm Ker}(A^T_{z\eta}\,M^{-1}_{zz})$ *parallel to* ${\rm Im}(A_{z\eta})$ *and the projector* $\mathbb{\Pi}^T$ *in* $\mathbb{R}^{N_z}$ *onto* ${\rm Ker}(A^T_{z\eta})$ *parallel to* ${\rm Im}(M^{-1}_{zz}A_{z\eta})$ *are defined by*

$$\mathbb{\Pi} = I - A_{z\eta}(A^T_{z\eta}M^{-1}_{zz}A_{z\eta})^{-1}A^T_{z\eta}M^{-1}_{zz}, \quad \mathbb{\Pi}^T = I - M^{-1}_{zz}A_{z\eta}(A^T_{z\eta}\,M^{-1}_{zz}\,A_{z\eta})^{-1}A^T_{z\eta}.$$

Moreover, we have $\mathbb{\Pi}A_{z\eta} = 0$, $\mathbb{\Pi}M_{zz} = M_{zz}\mathbb{\Pi}^T$, $M^{-1}_{zz}\mathbb{\Pi} = \mathbb{\Pi}^T\,M^{-1}_{zz}$.

Proof. The proof is standard and is left to the reader. ∎

As mentioned in the introduction, we have $N_\eta < N_z$ and we assume that $A_{z\eta}$ is of rank N_η. In that case the matrix $A_{z\eta}^T\, M_{zz}^{-1}\, A_{z\eta}$ is invertible, and the formulas in Proposition 3.1 are well defined. The fact that $A_{z\eta}$ is of rank N_η follows from the inf-sup condition stated in (4.3).

PROPOSITION 3.2. *Let* $\mathbf{v}$ *belong to* $H^1(0,\infty;\mathbb{R}^{N_c})$. *A pair* $(\mathbf{z},\boldsymbol{\eta})$ *is a solution of* (3.5) *if and only if* $(\mathbf{z},\boldsymbol{\eta})$ *is a solution to the system*

$$
\begin{aligned}
&\mathbb{\Pi}^T\mathbf{z}'(t) = \mathbb{\Pi}^T\, M_{zz}^{-1} A_{zz}\mathbb{\Pi}^T\mathbf{z}(t) + \mathbf{B}\,\mathbf{v}(t),\\
&(I-\mathbb{\Pi}^T)\mathbf{z}(t) = M_{zz}^{-1}A_{z\eta}(A_{z\eta}^T M_{zz}^{-1}A_{z\eta})^{-1}M_{\eta\eta}\,\mathbf{G}\,\mathbf{v}(t),\\
&\boldsymbol{\eta}(t) = (A_{z\eta}^T M_{zz}^{-1}A_{z\eta})^{-1}A_{z\eta}^T\mathbf{z}'(t) - (A_{z\eta}^T M_{zz}^{-1}A_{z\eta})^{-1}A_{z\eta}^T M_{zz}^{-1}A_{zz}\mathbf{z}(t),
\end{aligned}
\tag{3.6}
$$

where $\mathbf{A} = \mathbb{\Pi}^T M_{zz}^{-1}A_{zz} \in \mathbb{R}^{N_z\times N_z}$ *and* $\mathbf{B} = \mathbf{A}\, M_{zz}^{-1}A_{z\eta}(A_{z\eta}^T M_{zz}^{-1}A_{z\eta})^{-1}M_{\eta\eta}\,\mathbf{G}$.

Proof. By applying the discrete Leray projector $\mathbb{\Pi}$ to $(3.5)_1$, we obtain

$$\mathbb{\Pi}^T\mathbf{z}' = \mathbf{A}\mathbb{\Pi}^T\mathbf{z} + \mathbf{A}(I-\mathbb{\Pi}^T)\mathbf{z}.$$

From the expression of $(I-\mathbb{\Pi}^T)$ and from $(3.5)_2$, it follows that

$$(I-\mathbb{\Pi}^T)\mathbf{z} = M_{zz}^{-1}A_{z\eta}(A_{z\eta}^T M_{zz}^{-1}A_{z\eta})^{-1}M_{\eta\eta}\,\mathbf{G}\,\mathbf{v}.$$

The equation for $\boldsymbol{\eta}$ is obtained by multiplying $(3.5)_1$ by $A_{z\eta}^T M_{zz}^{-1}$, and next by $(A_{z\eta}^T M_{zz}^{-1}A_{z\eta})^{-1}$. Thus, we have proved that a solution $(\mathbf{z},\boldsymbol{\eta})$ of (3.5) is a solution to system (3.6). The converse statement can be established with similar calculations. ∎

From Proposition 3.2, it follows that only the initial condition $\mathbb{\Pi}^T\mathbf{z}(0)$ may be chosen to solve system (3.5) or (3.6). The only consistent initial condition for $(I-\mathbb{\Pi}^T)\mathbf{z}$ is

$$(I-\mathbb{\Pi}^T)\mathbf{z}(0) = M_{zz}^{-1}A_{z\eta}(A_{z\eta}^T M_{zz}^{-1}A_{z\eta})^{-1}M_{\eta\eta}\,\mathbf{G}\,\mathbf{v}(0).$$

Thus, the finite dimensional approximation of system (1.5) is

$$
\begin{aligned}
&M_{zz}\mathbf{z}'(t) = A_{zz}\mathbf{z}(t) + A_{z\eta}\boldsymbol{\eta}(t), \quad A_{z\eta}^T\mathbf{z}(t) - M_{\eta\eta}\,\mathbf{G}\,\mathbf{v}(t) = 0,\\
&\mathbf{z}(0) = \mathbb{\Pi}^T\mathbf{z}_0 + M_{zz}^{-1}A_{z\eta}(A_{z\eta}^T M_{zz}^{-1}A_{z\eta})^{-1}M_{\eta\eta}\,\mathbf{G}\,\mathbf{v}(0),
\end{aligned}
\tag{3.7}
$$

and we have proved the following theorem.

THEOREM 3.3. *Assume that* $\mathbf{v}$ *belong to* $H^1(0,\infty;\mathbb{R}^{N_c})$. *A pair* $(\mathbf{z},\boldsymbol{\eta})$ *is a solution of* (3.7) *if and only if* $(\mathbf{z},\boldsymbol{\eta})$ *is the solution to the system*

$$
\begin{aligned}
&\mathbb{\Pi}^T\mathbf{z}'(t) = \mathbf{A}\,\mathbb{\Pi}^T\mathbf{z}(t) + \mathbf{B}\mathbf{v}(t), \quad \mathbb{\Pi}^T\mathbf{z}(0) = \mathbb{\Pi}^T\mathbf{z}_0,\\
&(I-\mathbb{\Pi}^T)\mathbf{z}(t) = M_{zz}^{-1}A_{z\eta}(A_{z\eta}^T M_{zz}^{-1}A_{z\eta})^{-1}M_{\eta\eta}\,\mathbf{G}\,\mathbf{v}(t),\\
&\boldsymbol{\eta}(t) = (A_{z\eta}^T M_{zz}^{-1}A_{z\eta})^{-1}A_{z\eta}^T\mathbf{z}'(t) - (A_{z\eta}^T M_{zz}^{-1}A_{z\eta})^{-1}A_{z\eta}^T M_{zz}^{-1}A_{zz}\mathbf{z}(t).
\end{aligned}
\tag{3.8}
$$

Remark 3.4. We can verify that the semidiscrete approximation of (1.4) is

$$
\begin{aligned}
&M_{zz}\mathbf{z}'(t) = A_{zz}\mathbf{z}(t) + A_{z\eta}\boldsymbol{\eta}(t) + \mathcal{F}(\mathbf{z}(t)), \quad A_{z\eta}^T\mathbf{z}(t) - M_{\eta\eta}\mathbf{G}\,\mathbf{v}(t) = 0,\\
&\mathbf{z}(0) = \mathbb{\Pi}^T\mathbf{z}_0 + M_{zz}^{-1}A_{z\eta}(A_{z\eta}^T\, M_{zz}^{-1}\, A_{z\eta})^{-1}M_{\eta\eta}\,\mathbf{G}\,\mathbf{v}(0),\\
&\textit{with}\quad \mathcal{F}(\mathbf{z}(t)) = -\left(\sum_{k=1}^{N_z}\sum_{j=1}^{N_z} z_j\, z_k \int_\Omega (\phi_j\cdot\nabla)\phi_k\,\phi_i\,dx\right)_{1\le i\le N_z}.
\end{aligned}
\tag{3.9}
$$

3.3. Approximation of the complex eigenvalue problems. It is convenient to assume that $0 \notin \mathrm{spect}(\mathbf{A})$. If it is not the case, we can replace $\mathbf{A}$ by $\mathbf{A} - \lambda_0 I$ with $\lambda_0 \notin \mathrm{spect}(\mathbf{A})$ and introduce the corresponding obvious modifications in what follows. We know that

$$\mathbb{R}^{N_z} = \mathrm{Ker}(A_{z\eta}^T) \oplus \mathrm{Im}(M_{zz}^{-1} A_{z\eta}),$$

with $\mathrm{Ker}(A_{z\eta}^T) = \mathrm{Im}(\mathbb{\Pi}^T)$ and $\mathrm{Im}(M_{zz}^{-1} A_{z\eta}) = \mathrm{Ker}(\mathbb{\Pi}^T)$. Since $0 \notin \mathrm{spect}(\mathbf{A})$, we notice that $\mathrm{Im}(M_{zz}^{-1} A_{z\eta}) = \mathrm{Ker}\,(\mathbb{\Pi}^T) = \mathrm{Ker}\,(\mathbf{A}\,\mathbb{\Pi}^T)$. We look for a decomposition of $\mathbb{R}^{N_z}$ into the sum of generalized eigenspaces of the operator $\mathbf{A}\,\mathbb{\Pi}^T$. We denote by $(\boldsymbol{\lambda}_j)_{1 \le j \le N_e}$ the complex eigenvalues of the operator $\mathbf{A}\,\mathbb{\Pi}^T$. We already know that 0 is an eigenvalue of $\mathbf{A}\,\mathbb{\Pi}^T$ and that $\mathrm{Im}(M_{zz}^{-1} A_{z\eta}) = \mathrm{Ker}\,(\mathbf{A}\,\mathbb{\Pi}^T)$ is the corresponding eigenspace. In order to decompose $\mathrm{Ker}(A_{z\eta}^T)$ into the other generalized eigenspaces of the operator $\mathbf{A}\,\mathbb{\Pi}^T$, we consider the eigenvalue problem

$$\boldsymbol{\lambda} \in \mathbb{C}^*, \quad \mathbf{f} \in \mathrm{Ker}(A_{z\eta}^T), \quad \mathbf{f} \neq 0_{\mathbb{C}^{N_z}}, \quad \mathbf{A}\mathbf{f} = \boldsymbol{\lambda}\mathbf{f} \tag{3.10}$$

and the adjoint eigenvalue problem for $\mathbf{A}^\sharp = \mathbb{\Pi}^T M_{zz}^{-1} A_{zz}^T$,

$$\boldsymbol{\lambda} \in \mathbb{C}^*, \quad \boldsymbol{\phi} \in \mathrm{Ker}(A_{z\eta}^T), \quad \boldsymbol{\phi} \neq 0_{\mathbb{C}^{N_z}}, \quad \mathbf{A}^\sharp \boldsymbol{\phi} = \boldsymbol{\lambda}\boldsymbol{\phi}. \tag{3.11}$$

THEOREM 3.5. *A pair* $(\boldsymbol{\lambda}, \mathbf{f}) \in \mathbb{C}^* \times \mathbb{C}^{N_z}$ *is a solution to the eigenvalue problem* (3.10) *if and only if* $(\boldsymbol{\lambda}, \mathbf{f}, \boldsymbol{\eta}_{\mathbf{f}})$, *with* $\boldsymbol{\eta}_{\mathbf{f}} = (\mathbf{p}_{\mathbf{f}}, \boldsymbol{\tau}_{\mathbf{f}})^T = -(A_{z\eta}^T M_{zz} A_{z\eta})^{-1} A_{z\eta}^T M_{zz}^{-1} A_{zz}\,\mathbf{f}$, *is a solution to the eigenvalue problem*

$$\boldsymbol{\lambda} \in \mathbb{C}^*, \quad \mathbf{f} \in \mathbb{C}^{N_z}, \quad \mathbf{f} \neq 0_{\mathbb{C}^{N_z}}, \quad \boldsymbol{\eta}_{\mathbf{f}} \in \mathbb{C}^{N_\eta}, \quad A \begin{bmatrix} \mathbf{f} \\ \boldsymbol{\eta}_{\mathbf{f}} \end{bmatrix} = \boldsymbol{\lambda} M \begin{bmatrix} \mathbf{f} \\ \boldsymbol{\eta}_{\mathbf{f}} \end{bmatrix}, \tag{3.12}$$

where A *and* M *are the matrices defined in* (3.4). *Similarly,* $(\boldsymbol{\lambda}, \boldsymbol{\phi}) \in \mathbb{C}^* \times \mathbb{C}^{N_z}$ *is a solution to the eigenvalue problem* (3.11) *if and only if* $(\boldsymbol{\lambda}, \boldsymbol{\phi}, \boldsymbol{\eta}_{\boldsymbol{\phi}})$, *with* $\boldsymbol{\eta}_{\boldsymbol{\phi}} = (\mathbf{p}_{\boldsymbol{\phi}}, \boldsymbol{\tau}_{\boldsymbol{\phi}})^T = -(A_{z\eta}^T M_{zz} A_{z\eta})^{-1} A_{z\eta}^T M_{zz}^{-1} A_{zz}\,\boldsymbol{\phi}$, *is a solution to the adjoint eigenvalue problem*

$$\boldsymbol{\lambda} \in \mathbb{C}^*, \quad \boldsymbol{\phi} \in \mathbb{C}^{N_z}, \quad \boldsymbol{\phi} \neq 0_{\mathbb{C}^{N_z}}, \quad \boldsymbol{\eta}_{\boldsymbol{\phi}} \in \mathbb{C}^{N_\eta}, \quad A^T \begin{bmatrix} \boldsymbol{\phi} \\ \boldsymbol{\eta}_{\boldsymbol{\phi}} \end{bmatrix} = \boldsymbol{\lambda} M \begin{bmatrix} \boldsymbol{\phi} \\ \boldsymbol{\eta}_{\boldsymbol{\phi}} \end{bmatrix}. \tag{3.13}$$

Proof. The proof follows from the definition of $\mathbf{A}$ and the expression of $\mathbb{\Pi}^T$. □

A similar statement can be proved for the generalized eigenvectors of problems (3.10) and (3.12) and of problems (3.11) and (3.13). Let us recall that a vector $\mathbf{f}_k \in (\mathbb{C}^{N_z} \setminus \{0_{\mathbb{C}^{N_z}}\})$ is a generalized eigenvector for problem (3.10) associated with a solution $(\boldsymbol{\lambda}, \mathbf{f})$ of (3.10) when

$$\mathbf{f}_k \in \mathrm{Ker}(A_{z\eta}^T), \quad \mathbf{f}_k \neq 0_{\mathbb{C}^{N_z}}, \quad (\mathbf{A} - \boldsymbol{\lambda})^k \mathbf{f}_k = \mathbf{f} \quad \text{for some } k \in \mathbb{N}^*.$$

THEOREM 3.6. *There exist a basis* $(\mathbf{f}^1, \cdots, \mathbf{f}^{N_z})$ *of* $\mathbb{C}^{N_z}$ *constituted of eigenvectors and generalized eigenvectors of problem* (3.10) *and a basis* $(\boldsymbol{\phi}^1, \cdots, \boldsymbol{\phi}^{N_z})$ *of* $\mathbb{C}^{N_z}$ *constituted of eigenvectors and generalized eigenvectors of problem* (3.11) *satisfying the biorthogonality condition*

$$(\mathbf{f}^i)^T\, M_{zz}\, \boldsymbol{\phi}^j = \delta_{ij} \quad \textit{for } 1 \le i,\, j \le N_z.$$

If $\mathbf{F} \in \mathbb{C}^{N_z \times N_z}$ *is the matrix whose columns are* $(\mathbf{f}^1, \cdots, \mathbf{f}^{N_z})$ *and* $\mathbf{\Phi}$ *is the matrix whose columns are* $(\boldsymbol{\phi}^1, \cdots, \boldsymbol{\phi}^{N_z})$*, we have*

$$\Lambda_{\mathbb{C}} = \mathbf{F}^{-1}\, \mathbf{A}\, \mathbb{\Pi}^T\, \mathbf{F} \quad \textit{and} \quad \Lambda_{\mathbb{C}}^T = \Phi^{-1}\, \mathbf{A}^\sharp\, \mathbb{\Pi}^T\, \Phi,$$

where $\Lambda_{\mathbb{C}}$ *is a decomposition of* $\mathbf{A}\, \mathbb{\Pi}^T$ *into complex Jordan blocks.*

Proof. The proof is standard in linear algebra. ∎

3.4. Real biorthogonal families. Now, we are going to define two real biorthogonal families as explained hereafter. If $\boldsymbol{\lambda}_j$ is real and if $\mathbf{f}^k$ is an associated eigenvector or generalized eigenvector, we can assume that $\mathbf{f}^k$ and $\boldsymbol{\phi}^k$ are real vectors, and we set

$$(\mathbf{e}^k, \mathbf{p}_{\mathbf{e}^k}, \boldsymbol{\tau}_{\mathbf{e}^k}) = (\mathbf{f}^k, \mathbf{p}_{\mathbf{f}^k}, \boldsymbol{\tau}_{\mathbf{f}^k}), \quad (\boldsymbol{\xi}^k, \mathbf{p}_{\boldsymbol{\xi}^k}, \boldsymbol{\tau}_{\boldsymbol{\xi}^k}) = (\boldsymbol{\phi}^k, \mathbf{p}_{\boldsymbol{\phi}^k}, \boldsymbol{\tau}_{\boldsymbol{\phi}^k}).$$

If $\boldsymbol{\lambda}_j$ is a complex eigenvalue with $\operatorname{Im} \boldsymbol{\lambda}_j \neq 0$, then necessarily $\overline{\boldsymbol{\lambda}_j}$ is also an eigenvalue, and if $\mathbf{f}^k$ and $\boldsymbol{\phi}^k$ are associated eigenvectors or generalized eigenvectors, then we may assume that $\overline{\mathbf{f}^k} = \mathbf{f}^m$ and $\overline{\boldsymbol{\phi}^k} = \boldsymbol{\phi}^m$ (for some m) are eigenvectors or generalized eigenvectors associated with $\overline{\boldsymbol{\lambda}_j} = \boldsymbol{\lambda}_m$. In that case we set

$$\begin{aligned}
&(\mathbf{e}^k, \mathbf{p}_{\mathbf{e}^k}, \boldsymbol{\tau}_{\mathbf{e}^k}) = \sqrt{2}\operatorname{Re}(\mathbf{f}^k, \mathbf{p}_{\mathbf{f}^k}, \boldsymbol{\tau}_{\mathbf{f}^k}), \quad (\boldsymbol{\xi}^k, \mathbf{p}_{\boldsymbol{\xi}^k}, \boldsymbol{\tau}_{\boldsymbol{\xi}^k}) = \sqrt{2}\operatorname{Re}(\boldsymbol{\phi}^k, \mathbf{p}_{\boldsymbol{\phi}^k}, \boldsymbol{\tau}_{\boldsymbol{\phi}^k}) \quad \text{and} \\
&(\mathbf{e}^m, \mathbf{p}_{\mathbf{e}^m}, \boldsymbol{\tau}_{\mathbf{e}^m}) = \sqrt{2}\operatorname{Im}(\mathbf{f}^k, \mathbf{p}_{\mathbf{f}^k}, \boldsymbol{\tau}_{\mathbf{f}^k}), \quad (\boldsymbol{\xi}^m, \mathbf{p}_{\boldsymbol{\xi}^m}, \boldsymbol{\tau}_{\boldsymbol{\xi}^m}) = \sqrt{2}\operatorname{Im}(\boldsymbol{\phi}^k, \mathbf{p}_{\boldsymbol{\phi}^k}, \boldsymbol{\tau}_{\boldsymbol{\phi}^k}).
\end{aligned}$$

In this way, we have constructed two bases $(\mathbf{e}^1, \cdots, \mathbf{e}^{N_z})$ and $(\boldsymbol{\xi}^1, \cdots, \boldsymbol{\xi}^{N_z})$ of $\mathbb{R}^{N_z}$ satisfying the biorthogonality condition

$$(\mathbf{e}^i)^T\, M_{zz}\, \boldsymbol{\xi}^j = \delta_{ij} \quad \text{for } 1 \leq i,\, j \leq N_z.$$

Moreover, if $\mathbf{E} \in \mathbb{R}^{N_z \times N_z}$ is the matrix whose columns are $(\mathbf{e}^1, \cdots, \mathbf{e}^{N_z})$ and $\mathbf{\Xi} \in \mathbb{R}^{N_z \times N_z}$ is the matrix whose columns are the adjoint eigenvectors $(\boldsymbol{\xi}^1, \cdots, \boldsymbol{\xi}^{N_z})$, we have

$$\Lambda = \mathbf{E}^{-1}\, \mathbf{A}\, \mathbb{\Pi}^T\, \mathbf{E} \quad \text{and} \quad \Lambda^T = \mathbf{\Xi}^{-1}\, \mathbf{A}^\sharp\, \mathbb{\Pi}^T\, \mathbf{\Xi},$$

where Λ is a decomposition of $\mathbf{A}$ into real Jordan blocks. As in the previous section, we can also prove that

$$\Lambda = \mathbf{\Xi}^T\, A_{zz}\, \mathbb{\Pi}^T\, \mathbf{E} \quad \text{and} \quad \Lambda^T = \mathbf{E}^T\, \mathbb{\Pi}\, A_{zz}^T\, \mathbf{\Xi}.$$

We note that $\mathbf{A}^\sharp$ is not the transposed matrix of $\mathbf{A}$, while $\mathbf{\Xi}^{-1}\, \mathbf{A}^\sharp\, \mathbb{\Pi}^T\, \mathbf{\Xi}$ is actually the transposed matrix of Λ.

3.5. The projected dynamical system. In section 2.4, we have chosen Z_u and Z_u^* of the form

$$Z_u = \oplus_{j \in J_u} G_{\mathbb{R}}(\lambda_j) = \operatorname{vect}\{e_1, \cdots, e_{d_u}\}, \quad Z_u^* = \oplus_{j \in J_u} G_{\mathbb{R}}^*(\lambda_j) = \operatorname{vect}\{\xi_1, \cdots, \xi_{d_u}\}.$$

With the finite element approximation, the eigenvalues $(\lambda_j)_{j \in J_u}$ are approximated by $(\boldsymbol{\lambda}_j)_{j \in J_u}$, the functions $(e_i)_{1 \leq i \leq d_u}$ are approximated by $(\mathbf{e}_i)_{1 \leq i \leq d_u}$, and the functions $(\xi_i)_{1 \leq i \leq d_u}$ are approximated by $(\boldsymbol{\xi}_i)_{1 \leq i \leq d_u}$, where

$$\begin{aligned}
&\mathbf{e}_i = \textstyle\sum_{k=1}^{N_z} e_k^i\, \phi_k \quad \text{and} \quad \boldsymbol{\xi}_i = \textstyle\sum_{k=1}^{N_z} \xi_k^i\, \phi_k, \\
&\text{with} \quad (e_k^i)_{1 \leq k \leq N_z} = \mathbf{e}^i \quad \text{and} \quad (\xi_k^i)_{1 \leq k \leq N_z} = \boldsymbol{\xi}^i.
\end{aligned}$$

Thus, our method consists in approximating Z_u and Z_u^*, respectively, by

$$\mathbb{Z}_u = \oplus_{j\in J_u} G_{\mathbb{R}}(\boldsymbol{\lambda}_j) = \text{vect}\{\mathbf{e}^1, \cdots, \mathbf{e}^{d_u}\} \quad \text{and}$$
$$\mathbb{Z}_u^* = \oplus_{j\in J_u} G_{\mathbb{R}}^*(\boldsymbol{\lambda}_j) = \text{vect}\{\boldsymbol{\xi}^1, \cdots, \boldsymbol{\xi}^{d_u}\}.$$

In order to define the projected dynamical system that will be used in our stabilization strategy, it is convenient to introduce some notation. We denote by d_ℓ the dimension of $\text{Ker}\,(\mathbf{A}\,\mathbb{\Pi}^T)$, and we set $d_s = N_z - d_\ell - d_u$. We assume that $(\mathbf{e}^1, \cdots, \mathbf{e}^{N_z})$ are numbered in such a way that

$$\text{Ker}\,(\mathbf{A}\,\mathbb{\Pi}^T) = \text{Ker}\,(\mathbb{\Pi}^T) = \text{vect}\{\mathbf{e}^{d_u+d_s+1}, \cdots, \mathbf{e}^{N_z}\}.$$

We denote by $\mathbf{E}_u \in \mathbb{R}^{N_z\times d_u}$ the matrix whose columns are $(\mathbf{e}^1, \cdots, \mathbf{e}^{d_u})$, by $\mathbf{E}_s \in \mathbb{R}^{N_z\times d_s}$ the matrix whose columns are $(\mathbf{e}^{d_u+1}, \cdots, \mathbf{e}^{d_u+d_s})$, by $\boldsymbol{\Xi}_u \in \mathbb{R}^{N_z\times d_u}$ the matrix whose columns are $(\boldsymbol{\xi}^1, \cdots, \boldsymbol{\xi}^{d_u})$, and by $\boldsymbol{\Xi}_s \in \mathbb{R}^{N_z\times d_s}$ the matrix whose columns are $(\boldsymbol{\xi}^{d_u+1}, \cdots, \boldsymbol{\xi}^{d_u+d_s})$.

Then we set $\mathbb{Z}_s = \text{vect}\{\mathbf{e}^{d_u+1}, \cdots, \mathbf{e}^{N_z-d_\ell}\}$ and $\mathbb{K} = \text{vect}\{\mathbf{e}^{d_u+d_s+1}, \cdots, \mathbf{e}^{N_z}\} = \text{Ker}(\mathbb{\Pi}^T)$, and we have $\mathbb{R}^{N_z} = \mathbb{Z}_u \oplus \mathbb{Z}_s \oplus \mathbb{K}$. We introduce the operators $\mathbf{\Pi}_u \in \mathcal{L}(\mathbb{R}^{N_z}, \mathbb{Z}_u)$ and $\mathbf{\Pi}_s \in \mathcal{L}(\mathbb{R}^{N_z}, \mathbb{Z}_s)$ defined by

$$\mathbf{\Pi}_u = \mathbf{E}_u\,\boldsymbol{\Xi}_u^T\,M_{zz} \quad \text{and} \quad \mathbf{\Pi}_s = \mathbf{E}_s\,\boldsymbol{\Xi}_s^T\,M_{zz}.$$

PROPOSITION 3.7. *The operator $\mathbf{\Pi}_u$ is the projection onto $\mathbb{Z}_u$ parallel to $\mathbb{Z}_s \oplus \mathbb{K}$, and the operator $\mathbf{\Pi}_s$ is the projection onto $\mathbb{Z}_s$ parallel to $\mathbb{Z}_u \oplus \mathbb{K}$. Moreover, we have the following identities:*

$$\mathbf{\Pi}_u\mathbb{\Pi}^T = \mathbf{\Pi}_u, \quad \mathbf{\Pi}_s\mathbb{\Pi}^T = \mathbf{\Pi}_s, \quad \textit{and} \quad \mathbf{\Pi}_u + \mathbf{\Pi}_s = \mathbb{\Pi}^T.$$

Proof. The above statements, except the last one, follow from the biorthogonality property satisfied by $\mathbf{E}$ and $\boldsymbol{\Xi}$. The identity $\mathbf{\Pi}_u + \mathbf{\Pi}_s = \mathbb{\Pi}^T$ follows from the fact that both the operators $\mathbb{\Pi}^T$ and $\mathbf{\Pi}_u + \mathbf{\Pi}_s$ are the projection onto $\mathbb{Z}_u \oplus \mathbb{Z}_s$ parallel to $\mathbb{K}$. ∎

Let us note that the identity $\mathbf{\Pi}_u + \mathbf{\Pi}_s = \mathbb{\Pi}^T$ provides a very useful expression of $\mathbb{\Pi}^T$ that will be used in what follows. We also need the matrices of the Lagrange multipliers associated to the different families of eigenvectors introduced above. For that, we set $\mathbf{E}_{\eta,u} \in \mathbb{R}^{N_{\boldsymbol{\eta}}\times d_u}$ as the matrix whose columns are $(\boldsymbol{\eta}_{\mathbf{e}^1}, \cdots, \boldsymbol{\eta}_{\mathbf{e}^{d_u}})$, $\mathbf{E}_{\eta,s} \in \mathbb{R}^{N_{\boldsymbol{\eta}}\times d_s}$ as the matrix whose columns are $(\boldsymbol{\eta}_{\mathbf{e}^{d_u+1}}, \cdots, \boldsymbol{\eta}_{\mathbf{e}^{d_u+d_s}})$, $\boldsymbol{\Xi}_{\eta,u} \in \mathbb{R}^{N_{\boldsymbol{\eta}}\times d_u}$ as the matrix whose columns are $(\boldsymbol{\eta}_{\boldsymbol{\xi}^1}, \cdots, \boldsymbol{\eta}_{\boldsymbol{\xi}^{d_u}})$, and $\boldsymbol{\Xi}_{\eta,s} \in \mathbb{R}^{N_{\boldsymbol{\eta}}\times d_s}$ as the matrix whose columns are $(\boldsymbol{\eta}_{\boldsymbol{\xi}^{d_u+1}}, \cdots, \boldsymbol{\eta}_{\boldsymbol{\xi}^{d_u+d_s}})$. Let us recall that $\mathbf{E}_{\eta,u} = \left(\begin{smallmatrix}\mathbf{E}_{p,u}\\ \mathbf{E}_{\tau,u}\end{smallmatrix}\right)$. We have similar decompositions for $\mathbf{E}_{\eta,s}$, $\boldsymbol{\Xi}_{\eta,u}$, and $\boldsymbol{\Xi}_{\eta,s}$. We set

$$\Lambda_u = \boldsymbol{\Xi}_u^T\,A_{zz}\,\mathbf{E}_u, \qquad \Lambda_s = \boldsymbol{\Xi}_s^T\,A_{zz}\mathbf{E}_s. \tag{3.14}$$

Let us note that by definition

$$A\begin{pmatrix}\mathbf{E}_u\\ \mathbf{E}_{\eta,u}\end{pmatrix} = M\begin{pmatrix}\mathbf{E}_u\\ \mathbf{E}_{\eta,u}\end{pmatrix}\Lambda_u \quad \text{and} \quad A^T\begin{pmatrix}\boldsymbol{\Xi}_u\\ \boldsymbol{\Xi}_{\eta,u}\end{pmatrix} = M\begin{pmatrix}\boldsymbol{\Xi}_u\\ \boldsymbol{\Xi}_{\eta,u}\end{pmatrix}\Lambda_u^T. \tag{3.15}$$

Similar identities can be established for Λ_s.

Now, we have to explain how we can project the system (3.5) onto $\mathbb{Z}_u$. For that, we set

$$\mathbb{B}_u = -\boldsymbol{\Xi}_{\tau,u}^T M_{\tau\tau}\,\mathbf{G} \quad \text{and} \quad \mathbb{B}_s = -\boldsymbol{\Xi}_{\tau,s}^T M_{\tau\tau}\,\mathbf{G}. \tag{3.16}$$

PROPOSITION 3.8. *Let* $\mathbf{v}$ *belong to* $H^1(0,\infty;\mathbb{R}^{N_z})$. *If the pair* $(\mathbf{z},\boldsymbol{\eta})$ *is a solution of system* (3.7), *then the pair* $(\boldsymbol{\zeta}_u,\boldsymbol{\zeta}_s)$, *defined by*

$$\boldsymbol{\zeta}_u(t) = \boldsymbol{\Xi}_u^T M_{zz}\mathbf{z}(t), \quad \boldsymbol{\zeta}_s = \boldsymbol{\Xi}_s^T M_{zz}\mathbf{z}(t),$$

obeys the system

$$\begin{aligned} \boldsymbol{\zeta}_u'(t) &= \Lambda_u\,\boldsymbol{\zeta}_u(t) + \mathbb{B}_u\,\mathbf{v}(t), \quad \boldsymbol{\zeta}_u(0) = \boldsymbol{\Xi}_u^T M_{zz}\mathbf{z}_0, \\ \boldsymbol{\zeta}_s'(t) &= \Lambda_s\,\boldsymbol{\zeta}_s(t) + \mathbb{B}_s\,\mathbf{v}(t), \quad \boldsymbol{\zeta}_s(0) = \boldsymbol{\Xi}_s^T M_{zz}\mathbf{z}_0. \end{aligned} \tag{3.17}$$

Conversely, if $(\boldsymbol{\zeta}_u,\boldsymbol{\zeta}_s)$ *is a solution to system* (3.17), *then* $(\mathbf{z},\boldsymbol{\eta})$, *defined by*

$$\begin{aligned} \mathbf{z}(t) &= \mathbf{E}_u\,\boldsymbol{\zeta}_u(t) + \mathbf{E}_s\boldsymbol{\zeta}_s(t) + (I - \mathbb{\Pi}\mathbb{\Pi}^T)\,M_{zz}^{-1}A_{z\eta}(A_{z\eta}^T\,M_{zz}^{-1}\,A_{z\eta})^{-1}M_{\eta\eta}\,\mathbf{G}\,\mathbf{v}(t), \\ \boldsymbol{\eta}(t) &= (A_{z\eta}^T M_{zz}^{-1}A_{z\eta})^{-1}A_{z\eta}^T\mathbf{z}'(t) - (A_{z\eta}^T M_{zz}^{-1}A_{z\eta})^{-1}A_{z\eta}^T M_{zz}^{-1}A_{zz}\mathbf{z}(t), \end{aligned} \tag{3.18}$$

is a solution to system (3.7).

Proof. If we multiply $(3.5)_1$ by $\boldsymbol{\Xi}_u^T$ and $\boldsymbol{\Xi}_s^T$ and if we use the identities $\boldsymbol{\Xi}_u^T A_{z\eta} = 0$ and $\boldsymbol{\Xi}_s^T A_{z\eta} = 0$, we have

$$\boldsymbol{\Xi}_u^T\,M_{zz}\mathbf{z}'(t) = \boldsymbol{\Xi}_u^T\,A_{zz}\mathbf{z}(t) \quad \text{and} \quad \boldsymbol{\Xi}_s^T\,M_{zz}\mathbf{z}'(t) = \boldsymbol{\Xi}_s^T\,A_{zz}\mathbf{z}(t).$$

Using the identity $\boldsymbol{\Xi}_u^T\,A_{zz} + \boldsymbol{\Xi}_{\boldsymbol{\eta},u}^T\,A_{z\eta}^T = \Lambda_u\,\boldsymbol{\Xi}_u^T\,M_{zz}$, we obtain

$$\boldsymbol{\Xi}_u^T\,M_{zz}\,\mathbf{z}'(t) = \Lambda_u\,\boldsymbol{\Xi}_u^T\,M_{zz}\mathbf{z}(t) - \boldsymbol{\Xi}_{\boldsymbol{\eta},u}^T\,A_{z\eta}^T\mathbf{z}(t).$$

From the definition of $\boldsymbol{\zeta}_u$ and the equality $A_{z\eta}^T\mathbf{z}(t) = M_{\eta\eta}\mathbf{G}\,\mathbf{v}(t)$, it follows that

$$\boldsymbol{\zeta}_u'(t) = \Lambda_u\,\boldsymbol{\zeta}_u(t) - \boldsymbol{\Xi}_{\boldsymbol{\eta},u}^T\,M_{\eta\eta}\mathbf{G}\,\mathbf{v}(t).$$

Replacing $-\boldsymbol{\Xi}_{\boldsymbol{\eta},u}^T\,M_{\eta\eta}\mathbf{G}$ by $\mathbb{B}_u$, we recover the first equation in $(3.17)_1$. The equation for $\boldsymbol{\zeta}_s$ can be obtained in a similar way. With Proposition 3.7, the initial condition in (3.17) can be easily derived from the initial condition in (3.7). The first part of the proof is complete.

Let us now prove the converse statement. From the definition of $\mathbf{z}$ in (3.18) and from Proposition 3.7, it follows that $\mathbb{\Pi}\mathbb{\Pi}^T\mathbf{z} = \mathbf{E}_u\,\boldsymbol{\zeta}_u + \mathbf{E}_s\boldsymbol{\zeta}_s$ and

$$(I - \mathbb{\Pi}\mathbb{\Pi}^T)\mathbf{z} = (I - \mathbb{\Pi}\mathbb{\Pi}^T)\,M_{zz}^{-1}A_{z\eta}(A_{z\eta}^T\,M_{zz}^{-1}\,A_{z\eta})^{-1}M_{\eta\eta}\,\mathbf{G}\,\mathbf{v}.$$

Still with the definition of $\mathbf{z}$, we can easily verify that

$$\boldsymbol{\zeta}_u = \boldsymbol{\Xi}_u^T\,M_{zz}\mathbf{z}, \quad \boldsymbol{\zeta}_s = \boldsymbol{\Xi}_s^T\,M_{zz}\mathbf{z}, \quad \text{and} \quad A_{z\eta}^T\,\mathbf{z} = M_{\eta\eta}\,\mathbf{G}\,\mathbf{v}.$$

Now, knowing that $\boldsymbol{\zeta}_u$ and $\boldsymbol{\zeta}_s$ are the solutions to (3.17) and that $\mathbb{\Pi}\mathbb{\Pi}^T\mathbf{z} = \mathbf{E}_u\,\boldsymbol{\zeta}_u + \mathbf{E}_s\boldsymbol{\zeta}_s$, we have

$$\begin{aligned} \mathbb{\Pi}\mathbb{\Pi}^T\mathbf{z}' &= \mathbf{E}_u\,(\Lambda_u\,\boldsymbol{\zeta}_u - \boldsymbol{\Xi}_{\eta,u}^T\,A_{z\eta}^T\,\mathbf{z}) + \mathbf{E}_s(\Lambda_s\,\boldsymbol{\zeta}_s - \boldsymbol{\Xi}_{\eta,s}^T\,A_{z\eta}^T\,\mathbf{z}) \\ &= bE_u\,\boldsymbol{\Xi}_u^T\,M_{zz}M_{zz}^{-1}A_{zz}\,\mathbf{z} + \mathbf{E}_s\boldsymbol{\Xi}_s^T\,M_{zz}M_{zz}^{-1}A_{zz}\,\mathbf{z} \\ &= \mathbb{\Pi}\mathbb{\Pi}^T\,M_{zz}^{-1}A_{zz}\,\mathbf{z} = \mathbf{A}\,\mathbb{\Pi}\mathbb{\Pi}^T\mathbf{z} + \mathbf{B}\,\mathbf{v}. \end{aligned} \tag{3.19}$$

The initial condition in (3.7) can be recovered from the initial condition in (3.17). ∎

3.6. Stabilizability and feedback operator. We assume that the discrete approximation of the infinite dimensional eigenvalue problems is accurate enough so that the following holds:

(H_1)

For all $j \in J_u$, $\boldsymbol{\lambda}_j$ is an accurate approximation of λ_j,

for $1 \le i \le d_u$, $\mathbf{e}_i$ (resp., $\boldsymbol{\xi}_i$) is an accurate approximation of e_i (resp., ξ_i),

$-\alpha_s > \mathrm{Re\,spect}(\Lambda_s)$, $\mathbb{Z}_u$ and $\mathbb{Z}_u^*$ are of dimension d_u.

Remark 3.9. Verifying (H_1) is beyond the scope of the present paper. However, we have chosen a mesh fine enough so that any regular refinement of the mesh leads to the same results. The two unstable eigenvalues are obtained with a precision of order 10^{-4}, and the other first eight eigenvalues and their associated eigenvectors up to a precision of order 10^{-2}. According to the results reported in [11], computing the first 10 eigenvalues up to a precision of order 10^{-2} seems to be a good compromise between accuracy and computation time. We notice that this accuracy is sufficient to construct a feedback law able to stabilize the Navier–Stokes system (see section 6).

Due to Proposition 3.8, to stabilize system (3.5) it is necessary and sufficient to stabilize system (3.17). Due to assumption (H_1), $\Lambda_s \in \mathbb{R}^{d_s \times d_s}$ is stable. Thus, as will be shown in the proof of Theorem 3.11, to stabilize system (3.17), it is sufficient to stabilize the equation satisfied by $\boldsymbol{\zeta}_u$. This is why we make the following additional assumption:

(H_2) For all $\omega > -\mathrm{Re\,spect}(\Lambda_u)$, the pair $(\Lambda_u + \omega\, I_{\mathbb{R}^{d_u}}, \mathbb{B}_u)$ is stabilizable.

This is the discrete analogue of the condition for $(A_{\omega,u}, B_u)$ stated in (2.3).

Remark 3.10. If the family $(g_i)_{1 \le i \le N_c}$ is chosen so that the condition (2.3) is satisfied, and if (H_1) is satisfied, then the degree of stabilizability numerically determined in section 5.2 provides a numerical verification of (H_2) and (2.3).

Assuming that (H_2) is satisfied, for all $Q \in \mathcal{L}(\mathbb{R}^{d_u})$ satisfying $Q = Q^T \ge 0$ and for all $-\omega < \mathrm{Re\,spect}(\Lambda_u)$, the algebraic Riccati equation

$$\begin{aligned} &\mathbb{P}_{\omega,u} \in \mathcal{L}(\mathbb{R}^{d_u}), \quad \mathbb{P}_{\omega,u} = \mathbb{P}_{\omega,u}^T \ge 0, \quad \Lambda_u + \omega I_{\mathbb{R}^{d_u}} - \mathbb{B}_u \mathbb{B}_u^T \mathbb{P}_{\omega,u} \quad \text{is stable,} \\ &\mathbb{P}_{\omega,u}(\Lambda_u + \omega I_{\mathbb{R}^{d_u}}) + (\Lambda_u^T + \omega I_{\mathbb{R}^{d_u}})\mathbb{P}_{\omega,u} - \mathbb{P}_{\omega,u}\, \mathbb{B}_u \mathbb{B}_u^T \mathbb{P}_{\omega,u} + Q \;=\; 0 \end{aligned} \tag{3.20}$$

admits a unique solution. In the next section we are going to prove that the closed-loop system

$$\begin{aligned} &M_{zz}\mathbf{z}'(t) = A_{zz}\mathbf{z}(t) + A_{z\eta}\boldsymbol{\eta}(t), \\ &\mathbf{z}(0) = \mathbb{\Pi}^T \mathbf{z}_0 - M_{zz}^{-1} A_{z\eta}(A_{z\eta}^T M_{zz}^{-1} A_{z\eta})^{-1} M_{\eta\eta}\, \mathbf{G}\, \mathbb{B}_u^T \mathbb{P}_{\omega,u}\, \boldsymbol{\Xi}_u^T M_{zz}\mathbf{z}_0, \\ &A_{z\eta}^T \mathbf{z}(t) = -M_{\eta\eta}\mathbf{G}\, \mathbb{B}_u^T \mathbb{P}_{\omega,u}\, \boldsymbol{\Xi}_u^T M_{zz}\mathbf{z}(t) \end{aligned} \tag{3.21}$$

is stable. According to Theorem 3.11, system (3.21) is equivalent to

$$\begin{aligned} &\mathbb{\Pi}^T \mathbf{z}'(t) = \mathbf{A}\, \mathbb{\Pi}^T \mathbf{z}(t) - \mathbf{B}\, \mathbb{B}_u^T \mathbb{P}_{\omega,u}\, \boldsymbol{\Xi}_u^T M_{zz}\mathbf{z}(t), \quad \mathbb{\Pi}^T \mathbf{z}(0) = \mathbb{\Pi}^T \mathbf{z}_0, \\ &(I - \mathbb{\Pi}^T)\mathbf{z}(t) = -M_{zz}^{-1} A_{z\eta}(A_{z\eta}^T M_{zz}^{-1} A_{z\eta})^{-1} M_{\eta\eta}\, \mathbf{G}\, \mathbb{B}_u^T \mathbb{P}_{\omega,u}\, \boldsymbol{\Xi}_u^T M_{zz}\mathbf{z}(t), \\ &\boldsymbol{\eta}(t) = (A_{z\eta}^T M_{zz}^{-1} A_{z\eta})^{-1} A_{z\eta}^T \mathbf{z}'(t) - (A_{z\eta}^T M_{zz}^{-1} A_{z\eta})^{-1} A_{z\eta}^T M_{zz}^{-1} A_{zz}\mathbf{z}(t). \end{aligned} \tag{3.22}$$

Notice that in the right-hand side of $(3.21)_2$ only $\mathbb{\Pi}^T \mathbf{z}_0$ intervenes. Indeed, the term $\boldsymbol{\Xi}_u^T M_{zz}\mathbf{z}_0$ is nothing but the coordinate vector of $\mathbf{\Pi}_u \mathbf{z}_0 = \mathbf{\Pi}_u \mathbb{\Pi}^T \mathbf{z}_0$ in the basis $\mathbf{E}_u$.

This means that in $(3.21)_2$, the initial condition $\mathbf{z}(0)$ is entirely determined in terms of $\mathbb{\Pi}^T\mathbf{z}_0$.

If the linear feedback law is used in the nonlinear system (3.9), we obtain the following nonlinear closed-loop system:

$$\begin{aligned} &M_{zz}\mathbf{z}'(t) = A_{zz}\mathbf{z}(t) + A_{z\eta}\boldsymbol{\eta}(t) + \mathcal{F}(\mathbf{z}(t)),\\ &\mathbf{z}(0) = \mathbb{\Pi}^T\mathbf{z}_0 - M_{zz}^{-1}A_{z\eta}(A_{z\eta}^T\,M_{zz}^{-1}\,A_{z\eta})^{-1}M_{\eta\eta}\,\mathbf{G}\,\mathbb{B}_u^T\mathbb{P}_{\omega,u}\,\boldsymbol{\Xi}_u^T M_{zz}\mathbf{z}_0,\\ &A_{z\eta}^T\mathbf{z}(t) = -M_{\eta\eta}\mathbf{G}\,\mathbb{B}_u^T\mathbb{P}_{\omega,u}\,\boldsymbol{\Xi}_u^T M_{zz}\mathbf{z}(t). \end{aligned} \tag{3.23}$$

3.7. Stabilization results.

THEOREM 3.11. *The solution to the finite dimensional closed-loop system* (3.21) *obeys*

$$\begin{aligned} &\|\mathbf{\Pi}_u\mathbf{z}(t)\|_{\mathbb{R}^{d_u}} \le C\,e^{-\omega t}\|\mathbf{z}_0\|_{\mathbb{R}^{N_z}},\\ &\|(I-\mathbb{\Pi}^T)\mathbf{z}(t)\|_{\mathbb{R}^{d_\ell}} + \|\mathbf{\Pi}_s\mathbf{z}(t)\|_{\mathbb{R}^{d_s}} \le C\,e^{-\alpha_s t}\|\mathbf{z}_0\|_{\mathbb{R}^{N_z}}, \end{aligned} \tag{3.24}$$

where α_s is the decay rate appearing in (H_1).

Proof. First recall that $\mathbf{\Pi}_u\mathbf{z} = \mathbf{E}_u\,\boldsymbol{\zeta}_u$, $\mathbf{\Pi}_s\mathbf{z} = \mathbf{E}_s\,\boldsymbol{\zeta}_s$, with $(\boldsymbol{\zeta}_u,\boldsymbol{\zeta}_s) = (\boldsymbol{\Xi}_u^T M_{zz}\mathbf{z}$, $\boldsymbol{\Xi}_s^T M_{zz}\mathbf{z})$, and that

$$(I-\mathbb{\Pi}^T)\mathbf{z} = (I-\mathbb{\Pi}^T)\,M_{zz}^{-1}A_{z\eta}(A_{z\eta}^T\,M_{zz}^{-1}\,A_{z\eta})^{-1}M_{\eta\eta}\mathbf{G}\,\mathbb{B}_u^T\mathbb{P}_{\omega,u}\,\boldsymbol{\zeta}_u.$$

From Proposition 3.8, it follows that the pair $(\boldsymbol{\zeta}_u,\boldsymbol{\zeta}_s)$ obeys the system

$$\begin{pmatrix}\boldsymbol{\zeta}_u\\ \boldsymbol{\zeta}_s\end{pmatrix}' = \begin{pmatrix}\Lambda_u - \mathbb{B}_u\,\mathbb{B}_u^T\mathbb{P}_{\omega,u} & 0\\ -\mathbb{B}_s\,\mathbb{B}_u^T\mathbb{P}_{\omega,u} & \Lambda_s\end{pmatrix}\begin{pmatrix}\boldsymbol{\zeta}_u\\ \boldsymbol{\zeta}_s\end{pmatrix}, \quad \begin{pmatrix}\boldsymbol{\zeta}_u\\ \boldsymbol{\zeta}_s\end{pmatrix}(0) = \begin{pmatrix}\boldsymbol{\Xi}_u^T M_{zz}\mathbf{z}_0\\ \boldsymbol{\Xi}_s^T M_{zz}\mathbf{z}_0\end{pmatrix}. \tag{3.25}$$

Since

$$\|e^{t(\Lambda_u-\mathbb{B}_u\,\mathbb{B}_u^T\mathbb{P}_{\omega,u})}\|_{\mathcal{L}(\mathbb{R}^{d_u})} \le C\,e^{-\omega t} \quad\text{and}\quad \|e^{t\,\Lambda_s}\|_{\mathcal{L}(\mathbb{R}^{d_s})} \le C\,e^{-\alpha_s t} \quad \text{for all } t\ge 0,$$

the proof can be easily derived from these estimates. ∎

THEOREM 3.12. *Let α_s be the decay rate appearing in (H_1). Assume that (H_2) is satisfied and that, in addition, $\omega \ge \alpha_s$. There exist constants $C_0 > 0$ and $C_1 \ge 1$ such that for all $C \in (0, C_0)$ and all $\mathbf{z}_0 \in \mathbb{R}^{N_z}$ obeying $\|\mathbb{\Pi}^T\mathbf{z}_0\|_{\mathbb{R}^{N_z}} \le C/C_1$, the finite dimensional closed-loop nonlinear system* (3.23) *admits a unique solution in the space*

$$\Big\{\mathbf{z} \in H^1(0,\infty;\mathbb{R}^{N_z}) \mid \|e^{-\alpha_s t}\mathbf{z}(t)\|_{\mathbb{R}^{N_z}} \le C\Big\}.$$

In particular the solution to system (3.23) *obeys $\|\mathbf{z}(t)\|_{\mathbb{R}^{N_z}} \le C\,e^{-\alpha_s t}$.*

Proof. The proof can be completed by a fixed point method as in [26, Proof of Theorem 4.2]. ∎

Let us now recall some results useful in defining the best control location and the degree of stabilizability for the controlled system projected onto an invariant subspace.

PROPOSITION 3.13. *Let $\omega \ge 0$ be such that $-\omega < \mathrm{Re\,spect}(\Lambda_u)$. The following statements are equivalent:*

(i) *The pair $(\Lambda_u + \omega I_{\mathbb{R}^{d_u}}, \mathbb{B}_u)$ is stabilizable.*

(ii) *The stabilizability Gramian* $\mathbb{G}_{\omega,u}$*, of the pair* $(-\Lambda_u - \omega I_{\mathbb{R}^{d_u}}, \mathbb{B}_u)$*, satisfies*

$$\mathbb{G}_{\omega,u} = \int_0^\infty e^{-t(\Lambda_u+\omega I_{\mathbb{R}^{d_u}})}\, \mathbb{B}_u\, \mathbb{B}_u^T e^{-t(\Lambda_u^T+\omega I_{\mathbb{R}^{d_u}})}\, dt \geq \alpha I_{\mathbb{R}^{d_u}}, \quad \textit{with } \alpha > 0. \tag{3.26}$$

(iii) *For* $Q = 0$*, the Riccati equation* (3.20) *admits a solution* $\mathbb{P}_{\omega,u}$ *which satisfies*

$$\mathbb{P}_{\omega,u} = (\mathbb{G}_{\omega,u})^{-1} \quad \textit{and} \quad 0 < \mathbb{P}_{\omega,u} \leq \beta I_{\mathbb{R}^{d_u}}, \quad \textit{with } \beta > 0. \tag{3.27}$$

Proof. The equivalence of (i)–(iii) follows from [21, Theorems 1 and 2]. □

The greatest eigenvalue of $\mathbb{P}_{\omega,u}$ (β in (3.27)) is a good indicator of the stabilizability of the pair $(\Lambda_u + \omega I_{\mathbb{R}^{d_u}}, \mathbb{B}_u)$. However, the greatest eigenvalue of $\mathbb{P}_{\omega,u}$ depends on the biorthogonal bases of $\mathbb{Z}_u$ and $\mathbb{Z}_u^*$. In order to have a criterion depending only on $\mathbb{Z}_u$ and $\mathbb{Z}_u^*$, but independent of their bases, we have to come back to a criterion defined for the infinite dimensional system and for its numerical approximation.

We define the degree of stabilizability of the pair $(\Lambda_u+\omega I_{\mathbb{R}^{d_u}}, \mathbb{B}_u)$ as the numerical approximation of the smallest eigenvalue of the Gramian

$$G_{\omega,u} = \int_0^\infty e^{-t(A_u+\omega I)} B_u\, B_u^*\, e^{-t(A_u^*+\omega I)}\, dt,$$

where $B_u = \pi_u\, B$. Since $Z_u^* = \mathrm{vect}\{\xi_1, \cdots, \xi_{d_u}\}$ (see section 3.5), we have to determine

$$\begin{aligned} &\min \mathrm{spect}(G_{\omega,u}) \\ &= \inf\Big\{ \textstyle\int_0^\infty |B_u^*\, e^{-t(A_u^*+\omega I)} \sum_{\ell=1}^{d_u} \zeta_\ell \xi_\ell|^2_{\mathbb{R}^{N_c}}\, dt \mid \| \sum_{\ell=1}^{d_u} \zeta_\ell \xi_\ell \|_{L^2(\Omega)} = 1 \Big\}. \end{aligned} \tag{3.28}$$

The numerical approximations of $B_u^*\, e^{-t(A_u^*+\omega I)} \sum_{\ell=1}^{d_u} \zeta_\ell \xi_\ell$ and $\| \sum_{\ell=1}^{d_u} \zeta_\ell \xi_\ell \|^2_{L^2(\Omega)}$ are, respectively,

$$\mathbb{B}_u^T\, e^{-t(\Lambda_u^T+\omega I)}\, \zeta_u \quad \text{and} \quad \zeta_u^T\, \boldsymbol{\Xi}_u^T M_{zz} \boldsymbol{\Xi}_u\, \zeta_u,$$

where $\zeta_u = (\zeta_1, \cdots, \zeta_{d_u})^T$. Thus, due to (3.16), we have to consider the operator

$$\int_0^\infty e^{-t(\Lambda_u+\omega I)}\, \boldsymbol{\Xi}_{\tau,u}^T\, M_{\tau\tau}\, \mathbf{G}\, \mathbf{G}^T\, M_{\tau\tau}\, \boldsymbol{\Xi}_{\tau,u}\, e^{-t(\Lambda_u^T+\omega I)}\, dt = (\mathbb{P}_{\omega,u})^{-1}.$$

The minimization problem in (3.28) is approximated by

$$\inf\Big\{ \zeta_u^T \mathbb{P}_{\omega,u}^{-1} \zeta_u \mid \zeta_u^T\, \boldsymbol{\Xi}_u^T M_{zz} \boldsymbol{\Xi}_u\, \zeta_u = 1 \Big\}. \tag{3.29}$$

We approximate the smallest eigenvalue of the Gramian $G_{\omega,u}$ by $(\max \mathrm{spect}(\mathbb{S}_{\omega,u}))^{-1}$, where

$$\mathbb{S}_{\omega,u} = \mathbb{W}_u\, \mathbb{P}_{\omega,u}\, \mathbb{W}_u \quad \text{and} \quad \mathbb{W}_u = \big(\boldsymbol{\Xi}_u^T M_{zz} \boldsymbol{\Xi}_u\big)^{1/2}. \tag{3.30}$$

Similarly, we can define the degree of stabilizability for any finite dimensional invariant subspace. For any nonzero eigenvalue $\boldsymbol{\lambda}_j$ of $\mathbf{A}\boldsymbol{\Pi}^T$, there exists a family of indices $J_{\boldsymbol{\lambda}_j}$ such that

$$\mathbb{Z}_j = G_{\mathbb{R}}(\boldsymbol{\lambda}_j) = \mathrm{vect}\{\mathbf{e}^k \mid k \in J_{\boldsymbol{\lambda}_j}\} \quad \text{and} \quad \mathbb{Z}_j^* = G_{\mathbb{R}}^*(\boldsymbol{\lambda}_j) = \mathrm{vect}\{\boldsymbol{\xi}^k \mid k \in J_{\boldsymbol{\lambda}_j}\},$$

where $m_j = \dim(G_{\mathbb{R}}(\boldsymbol{\lambda}_j))$. We denote by $\mathbf{E}_j \in \mathbb{R}^{N_z \times m_j}$ the matrix whose columns are $(\mathbf{e}^k)_{k \in J_{\boldsymbol{\lambda}_j}}$, by $\boldsymbol{\Xi}_j$ the matrix whose columns are $(\boldsymbol{\xi}^k)_{k \in J_{\boldsymbol{\lambda}_j}}$, by $\mathbf{E}_{\eta,j} \in \mathbb{R}^{N_{\boldsymbol{\eta}} \times m_j}$

the matrix whose columns are $(\boldsymbol{\eta}_{\mathbf{e}^k})_{k\in J_{\boldsymbol{\lambda}_j}}$, and by $\boldsymbol{\Xi}_{\eta,j} \in \mathbb{R}^{N_{\boldsymbol{\eta}}\times m_j}$ the matrix whose columns are $(\boldsymbol{\eta}_{\boldsymbol{\xi}^k})_{k\in J_{\boldsymbol{\lambda}_j}}$. We set $\mathbb{B}_j = -\boldsymbol{\Xi}_{\boldsymbol{\eta},j}^T M_{\eta\eta}\mathbf{G}$ and $\Lambda_j = \boldsymbol{\Xi}_j^T A_{zz}\mathbf{E}_j$.

For any $\omega > \mathrm{Re}(\boldsymbol{\lambda}_j)$, if the pair $(\Lambda_j + \omega I_{\mathbb{R}^{m_j}}, \mathbb{B}_j)$ is stabilizable, then there exists a unique $\mathbb{P}_{\omega,j}$ solving the following Riccati equation:

$$\begin{aligned} &\mathbb{P}_{\omega,j} \in \mathcal{L}(\mathbb{R}^{m_j}), \quad \mathbb{P}_{\omega,j} = \mathbb{P}_{\omega,j}^T > 0, \\ &\mathbb{P}_{\omega,j}(\Lambda_j + \omega I_{\mathbb{R}^{m_j}}) + (\Lambda_j^T + \omega I_{\mathbb{R}^{m_j}})\mathbb{P}_{\omega,j} - \mathbb{P}_{\omega,j}\,\mathbb{B}_j\mathbb{B}_j^T\mathbb{P}_{\omega,j} = 0. \end{aligned} \tag{3.31}$$

We set $\mathbb{W}_j = \left(\boldsymbol{\Xi}_j^T M_{zz}\boldsymbol{\Xi}_j\right)^{1/2}$, and we define the degree of stabilizability of $G_{\mathbb{R}}(\boldsymbol{\lambda}_j)$ by

$$d_j = \left(\max \mathrm{spect}(\mathbb{W}_j\,\mathbb{P}_{\omega,j}\mathbb{W}_j)\right)^{-1}. \tag{3.32}$$

Remark 3.14. When $m_j = 1$, then $\boldsymbol{\Xi}_j$ is reduced to a unique vector $\boldsymbol{\xi}^{k_j}$ and $\mathbb{P}_{\omega,j}$ is a positive real number. If $\boldsymbol{\xi}^{k_j}$ is normalized, i.e., if $(\boldsymbol{\xi}^{k_j})^T M_{zz}\boldsymbol{\xi}^{k_j} = 1$, then $d_j = (\mathbb{P}_{\omega,j})^{-1}$.

When $m_j = 2$, which corresponds to the case of two complex conjugate eigenvalues, then $\boldsymbol{\Xi}_j = [\boldsymbol{\xi}_1^{k_j}\ \boldsymbol{\xi}_2^{k_j}]$, and

$$\mathbb{W}_j = \begin{pmatrix} 1 & \boldsymbol{\xi}_1^{k_j}\,M_{zz}\,\boldsymbol{\xi}_2^{k_j} \\ \boldsymbol{\xi}_1^{k_j}\,M_{zz}\,\boldsymbol{\xi}_2^{k_j} & 1 \end{pmatrix}^{1/2}$$

if the two vectors $\boldsymbol{\xi}_1^{k_j}$ and $\boldsymbol{\xi}_2^{k_j}$ are normalized.

4. Numerical approximation of the eigenvalue problem.

4.1. Data of numerical experiments. Let us introduce the data used in the numerical experiments. The parabolic velocity profile in the inflow boundary $\Gamma_i = \{-1.5\} \times [0, 0.4]$ is defined by

$$u_s(-1.5, x_2) = (u_s^1, u_s^2)^T = \left(6\left(\frac{x_2}{0.4}\left(1 - \frac{x_2}{0.4}\right)\right), 0\right)^T. \tag{4.1}$$

The mean value of u_s^1 is $U_m = 1$, and its maximal amplitude is 1.5. The Reynolds number $R_e = \frac{2r_c U_m}{\nu} = \frac{1}{10\nu}$ depends only on ν (see section 2.1).

Actuators. We parametrize the positions on the circle Γ_c by the angular position counterclockwise, with $\theta = 0°$ at $(0.3, 0.2)$. For the numerical tests, we choose $N_c = 2$. For a given $\theta \in (5°, 175°)$, the functions g_1^θ and g_2^θ in (1.3) are localized, respectively, in $I_1^\theta = [\theta - 5°, \theta + 5°]$ and $I_2^\theta = [-\theta - 5°, -\theta + 5°]$. They are represented below and defined by

$$\begin{aligned} &g_k^\theta(\vartheta) = g\left(\tfrac{\vartheta + (-1)^k\theta}{10} + \tfrac{1}{2}\right)(\cos(\vartheta), \sin(\vartheta))^T, \\ &g(s) = G(10s) - G(10(s-1)+1), \end{aligned} \tag{4.2}$$

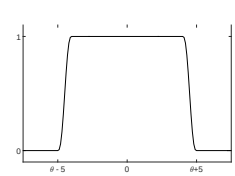

where $k = 1$ or $k = 2$, the control is acting only in the normal direction, and $G(s) = 0$ if $s \le 0$, $G(s) = s^3(6s^2 - 15s + 10)$ if $0 < s < 1$, and $G(s) = 1$ if $s \ge 1$.

Mesh and finite element approximation. The velocity, the pressure, and the Lagrange multiplier of Dirichlet boundary conditions are approximated with a P_3–P_2–P_3 finite element method. We assume that the triangulations defining X_h, M_h, and S_h satisfy the following inf-sup condition:

$$\inf_{(\psi,\zeta)\in M_h\times S_h,\,(\psi,\zeta)\neq 0}\ \sup_{z\in X_h,\,z\neq 0} \frac{b(z,\psi)-\langle\zeta,z\rangle_{\Gamma_c}}{\|z\|_{X_h}\,\|(\psi,\zeta)\|_{M_h\times S_h}} \geq \beta \tag{4.3}$$

for some $\beta > 0$ independent of h. With the same type of proof as in [17, Proposition 5], condition (4.3) will be satisfied if (X_h, M_h) satisfies another inf-sup condition of the form

$$\inf_{\psi\in M_h,\,\psi\neq 0}\ \sup_{z\in X_h,\,z\neq 0} \frac{b(z,\psi)}{\|z\|_{X_h}\,\|\psi\|_{M_h}} \geq \beta_0 > 0, \tag{4.4}$$

and provided that $h_s \geq K h_x$ with $K > 1$, where h_s is the mesh size of S_h and h_x is the mesh size of X_h. In [28], several situations, in which the constant K can be chosen close to 1, are analyzed.

Condition (4.4) for P_3-P_2 elements follows from the general result [33, Theorem 2.1] and from [33, Lemma 3.1].

The mesh used in the numerical tests consists of 8779 nodes. It is symmetric with respect to the horizontal axis of the cylinder, and it is plotted in Figure 2.1. The total number of degrees of freedom is 192386. The mesh on Γ_d used for S_h is that induced by the mesh on $\overline{\Omega}$. We have also realized numerical tests with finer meshes. Some comparisons are reported at the end of section 6.3.

Time solver. The time discretization is treated by a classical backward difference formula of order 2 (BDF2) with a time step $\Delta t = 10^{-3}$. A Newton algorithm is employed to treat the nonlinearity. At each time step iteration, we have to invert a matrix of the form

$$M - \frac{2\Delta t}{3}(A - BK) \quad \text{with} \quad B = \begin{pmatrix} 0 \\ M_{\eta\eta}\mathbf{G} \end{pmatrix} \quad \text{and} \quad K = \begin{pmatrix} -\mathbb{B}_u^T\mathbb{P}_{\omega,u}\,\boldsymbol{\Xi}_u^T M_{zz} & 0 \end{pmatrix}.$$

This matrix is inverted with the "MUMPS" solver. The numerical tests were realized with two different codes, one based on the free GetFEM++ library [32] and the other one on the COMSOL software [15]. The comparison between the two simulations gives us a higher reliability in the numerical results. The two codes give the same results.

4.2. Eigenvalue approximation. To capture the leading eigenvalues of problems (3.12) and (3.13), we use an Arnoldi method combined with a "shift and inverse" transformation implemented in the ARPACK library [22]. We fix the shift parameter at 10 and the size of the small Hessenberg matrix at 400.

For Reynolds numbers R_e in the range $[50, 255]$, the spectrum is characterized by two complex conjugate unstable eigenvalues (i.e., eigenvalues of strictly positive real parts) [7]. For $R_e = 150$, we have plotted in Figure 4.1 the nearest eigenvalues to the imaginary axis (the two unstable eigenvalues $\boldsymbol{\lambda}_1$ and $\boldsymbol{\lambda}_2 = \overline{\boldsymbol{\lambda}_1}$ are circled), and we report the ten eigenvalues close to the imaginary axis in Table 4.1.

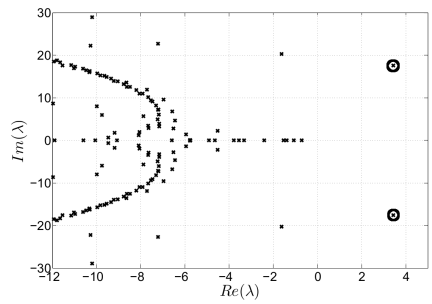

FIG. 4.1. *Eigenvalues of the linearized Navier–Stokes operator for* $R_e = 150$.

TABLE 4.1
First eigenvalues of the spectrum of $\mathbf{A}\,\mathbb{II}^T$ *for* $R_e = 150$.

i	1–2	3	4	5	6	7–8	9	10
$\boldsymbol{\lambda}_i$	$3.44 \pm 17.59i$	-0.71	-1.07	-1.38	-1.54	$-1.62 \pm 20.22i$	-2.41	-3.32

5. Best actuator location and degree of stabilizability.

5.1. Best actuator location. The control operator $\mathbb{B}_u$ in system $(3.17)_1$ depends on θ. Let us denote it by $\mathbb{B}_u^\theta$. We determine the best control location θ_{opt} by looking for the location which maximizes the *degree of stabilizability of the pair* $(\Lambda_u + \omega I_{\mathbb{R}^{d_u}}, \mathbb{B}_u)$. Thus, we have to solve the following min-max problem:

$$\theta_{\text{opt}} = \arg\min_\theta \max \text{ spect}\left(\mathbb{W}_u\, \mathbb{P}^\theta_{\omega,u}\, \mathbb{W}_u\right), \tag{5.1}$$

where $\mathbb{P}^\theta_{\omega,u}$ is the solution of (3.20) for $Q = 0$ and $\mathbb{W}_u$ is defined in (3.30).

We know that the control $v^\theta = -(\mathbb{B}_u^\theta)^T\, \mathbb{P}^\theta_{\omega,u}\, \boldsymbol{\zeta}_u$ corresponding to closed-loop system (3.25) obeys

$$\|e^{\omega\, t} v^\theta\|_{L^2(0,\infty;\mathbb{R}^{N_c})} = \boldsymbol{\zeta}_u(0)^T\, \mathbb{P}^\theta_{\omega,u}\, \boldsymbol{\zeta}_u(0).$$

Therefore, the best control location θ_{opt} is also the location which provides a control v^θ of minimal $L^2(0,\infty; e^{\omega\,\cdot})$-norm, among the controls $v \in L^2(0,\infty; e^{\omega\,\cdot})$ stabilizing the system

$$\boldsymbol{\zeta}'(t) = (\Lambda_u + \omega I_{\mathbb{R}^{d_u}})\boldsymbol{\zeta}(t) + \mathbb{B}_u^\theta v(t),$$

in the case of the worst initial condition $\boldsymbol{\zeta}(0) = \boldsymbol{\zeta}_u(0)$ satisfying the normalization condition $|\mathbb{W}_u^{-1}\boldsymbol{\zeta}_u(0)|_{\mathbb{R}^{d_u}} = 1$. (See also [25, page 451] for other criteria.)

We have calculated the best optimal control zone by choosing $\mathbb{Z}_u = G_{\mathbb{R}}(\boldsymbol{\lambda}_1)$. The matrix Λ_u is reduced to

$$\Lambda_u = \begin{bmatrix} \text{Re}(\boldsymbol{\lambda}_1) & \text{Im}(\boldsymbol{\lambda}_1) \\ -\text{Im}(\boldsymbol{\lambda}_1) & \text{Re}(\boldsymbol{\lambda}_1) \end{bmatrix}. \tag{5.2}$$

In Figure 5.1, we plot $\theta_{\text{opt}}(R_e)$ in terms of the Reynolds number $R_e \in [80, 255]$. We observe that the optimal location of the actuator moves away from the detachment zone of the flow on the cylinder's boundary (see [27], where θ is chosen equal to $70°$ for $R_e = 80$).

For $R_e = 150$ the optimal location of the actuators is $\theta_{\text{opt}}(150) = 95°$.

In the min-max problem (5.1), used to determine the best control location, we have chosen $\mathbb{Z}_u = G_{\mathbb{R}}(\boldsymbol{\lambda}_1)$ and $\omega = 0$. Other choices are possible. We have performed

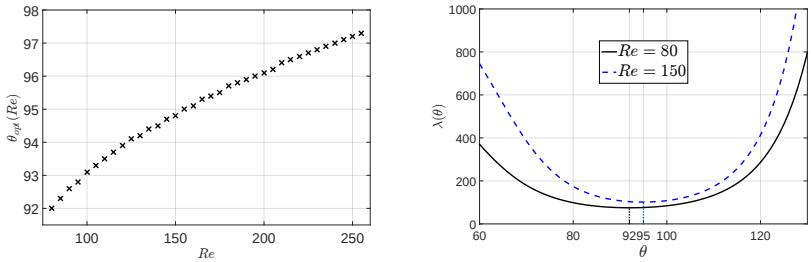

(a) $\theta_{\rm opt}(R_e)$ for $R_e \in [80, 255]$. (b) max spect $\big(\mathbb{W}_u\, \mathbb{P}^{\theta}_{0,u}\, \mathbb{W}_u\big)$.

FIG. 5.1. *Influence of Reynolds number on the optimal location of actuators.*

other numerical simulations for finding the best location with $\mathbb{Z}_u = G_{\mathbb{R}}(\boldsymbol{\lambda}_1) \oplus G_{\mathbb{R}}(\boldsymbol{\lambda}_7)$ and $\omega = 6$. Still in that case, we find nearly the same optimal value for $\theta_{\rm opt}$, up to a variation of one degree. The best location depends mainly on R_e and much less on ω and $\mathbb{Z}_u$. We think that this behavior is particular to our problem and is not a general fact.

For a review of the strategies used in the literature to determine the best actuator locations, we refer the reader to [24, 34, 25]. The H_2 optimal actuator location studied in [13] is covered by the general approach introduced in [25]. See also [20], where other strategies for the optimal actuator placement are proposed.

5.2. Degree of stabilizability. In Table 5.1, we report the numerical results obtained for the degree of stabilizability d_j of the subspaces $G_{\mathbb{R}}(\boldsymbol{\lambda}_j)$, as defined in (3.32), for $1 \le j \le 10$ and $\omega = 6$. We can notice that, except for $G_{\mathbb{R}}(\boldsymbol{\lambda}_1)$ and $G_{\mathbb{R}}(\boldsymbol{\lambda}_7)$, the other eigenspaces are weakly stabilizable. Therefore it is not necessarily a good strategy to include the corresponding eigenvectors in $\mathbb{Z}_u$.

TABLE 5.1
Degree of stabilizability of different eigenspaces for $R_e = 150$, $\omega = 6$, and d_j defined by (3.32).

$\boldsymbol{\lambda}_j$	$\boldsymbol{\lambda}_1$, $\boldsymbol{\lambda}_2$	$\boldsymbol{\lambda}_3$	$\boldsymbol{\lambda}_4$	$\boldsymbol{\lambda}_5$	$\boldsymbol{\lambda}_6$	$\boldsymbol{\lambda}_7$, $\boldsymbol{\lambda}_8$	$\boldsymbol{\lambda}_9$	$\boldsymbol{\lambda}_{10}$
$10^4 d_j$	15.14	$4.15\,10^{-2}$	$3.6\,10^{-7}$	$8.1\,10^{-3}$	$3.1\,10^{-3}$	8.45	$1.69\,10^{-2}$	$6.8\,10^{-4}$

6. Closed-loop Navier–Stokes system. For a Reynolds number relatively close to the critical Reynolds number $R_{ec} \approx 50$, that is, for $R_e \in (70, 90)$, it is relatively easy to stabilize the Navier–Stokes equations. We refer the reader to [27], where simulations were done for $R_e = 60$. The situation is different for higher Reynolds number. In [18], simulations are performed for Reynolds number equal to 200 and to 1000, with three control zones and an optimal open-loop control reducing the drag but not obtaining a full stabilization. To the best of our knowledge, very few feedback stabilization results exist for Reynolds number higher than 100. In the present work, we choose $R_e = 150$. In that situation, the contribution of the nonlinear term becomes more significant, and the flow is more sensitive to perturbations.

Now, we present numerical simulations of the closed-loop system (3.21) in which $\mathbb{P}_{\omega,u}$ is replaced by the solution $\mathbb{P}_{\Delta_u,Q} \in \mathcal{L}(\mathbb{R}^{d_u})$ to the equation

$$\begin{aligned} &\mathbb{P}_{\Delta_u,Q} = \mathbb{P}^T_{\Delta_u,Q} \ge 0, \quad \Lambda_u + \Delta_u - \mathbb{B}_u\mathbb{B}_u^T\mathbb{P}_{\Delta_u,Q} \quad \text{is stable,} \\ &\mathbb{P}_{\Delta_u,Q}(\Lambda_u + \Delta_u) + (\Lambda_u^T + \Delta_u)\mathbb{P}_{\Delta_u,Q} - \mathbb{P}_{\Delta_u,Q}\,\mathbb{B}_u\mathbb{B}_u^*\mathbb{P}_{\Delta_u,Q} + Q = 0, \end{aligned} \tag{6.1}$$

where $\Delta_u \in \mathcal{L}(\mathbb{R}^{d_u})$ is a diagonal matrix of the form $\Delta_u = \mathrm{diag}((\omega_j\, I_{\mathbb{R}^{m_j}})_{j\in J_u})$, $Q = \mathrm{diag}((Q_j)_{j\in J_u})$, $Q_j \in \mathcal{L}(\mathbb{R}^{m_j})$, $Q_j = Q_j^T \geq 0$, $m_j = \dim(G_{\mathbb{R}}(\boldsymbol{\lambda}_j))$, and either $\omega_j > -\mathrm{Re}(\boldsymbol{\lambda}_j)$ or $Q_j > 0$. We notice that if $\Delta_u = \omega I_{\mathbb{R}^{d_u}}$, then $\mathbb{P}_{\Delta_u,Q}$ is nothing but the solution $\mathbb{P}_{\omega,u}$ of (3.20). Thus (6.1) is a generalization of (3.20) which is helpful in some numerical tests in section 6.4.

To test the efficiency of different feedback laws for the Navier–Stokes system, rather than taking a perturbation of the stationary solution w_s in the initial condition, we choose $w(0) = w_s$ in system (1.2) or, similarly, $z_0 = 0$ in system (1.5), and we introduce a boundary perturbation $v_d(x,t) = \mu(t)\, h(x)$ in the inflow boundary $\Gamma_i \times (0,\infty)$, localized in time, defined by

$$\mu(t) = \beta\, e^{-30(t-1)^2}, \quad h = (h_1, h_2), \quad \text{and} \quad h_1(x) = g_d(x)\sigma(\boldsymbol{\xi}_1(x), \mathbf{p}_{\boldsymbol{\xi}^1}(x))\mathbf{n}.\mathbf{n}, \tag{6.2}$$

where $\beta > 0$ is a parameter used to vary the amplitude of the perturbation. The term $\sigma(\boldsymbol{\xi}_1, \mathbf{p}_{\boldsymbol{\xi}^1})\mathbf{n}.\mathbf{n}$ corresponds to $\tau_{\boldsymbol{\xi}^1}.\mathbf{n}$, and g_d is a truncation function defined on Γ_i by $g_d(x) = G(20s) - G(20(s-0.4)+1)$ for $x \in [0, 0.4]$ and $G(s) = s^3(6s^2 - 15s + 10)$. We assume that $\boldsymbol{\xi}^1$ is normalized. Since $\boldsymbol{\xi}^1 = \sqrt{2}\,\mathrm{Re}(\boldsymbol{\phi}^1)$, $\boldsymbol{\xi}^2 = \sqrt{2}\,\mathrm{Im}(\boldsymbol{\phi}^1)$, and $\boldsymbol{\phi}^1$ is an eigenvector corresponding to the most unstable eigenvalues, $\sigma(\boldsymbol{\xi}_1, \mathbf{p}_{\boldsymbol{\xi}^1})\mathbf{n}.\mathbf{n}$ corresponds to one of the most destabilizing normal boundary perturbations; see Figure 6.1.

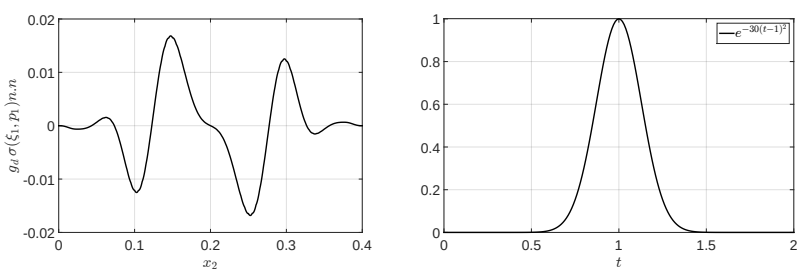

(a) Graph of h_1. (b) Graph of μ.

FIG. 6.1. *Inflow perturbation.*

In the following, we test different amplitudes β of the perturbation and different feedback laws by varying $\mathbb{Z}_u$, Δ_u, and Q. The norm of the uncontrolled solution for $\beta = 30$ is reported in Figure 6.2.

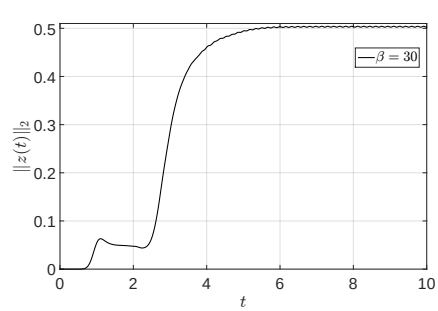

FIG. 6.2. *Evolution of the L^2-norm of the uncontrolled solution with $\beta = 30$.*

Since the perturbation h is symmetric with respect to the axis $x_2 = 0.2$, the feedback controls v_1 and v_2 (corresponding to the actuators g_1 and g_2, respectively)

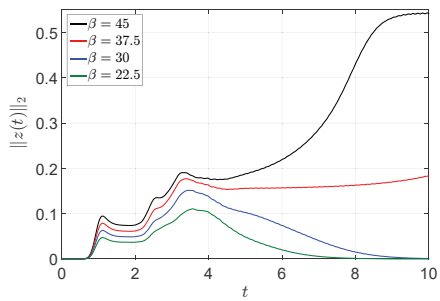

FIG. 6.3. *Evolution of the L^2-norm of the controlled solutions according to the amplitude β of the inflow perturbation* ($\mathbb{Z}_u = G_{\mathbb{R}}(\boldsymbol{\lambda}_1)$, $\Delta_u = \mathbf{0}_{\mathbb{R}^2}$, $Q = \mathbf{0}_{\mathbb{R}^2}$).

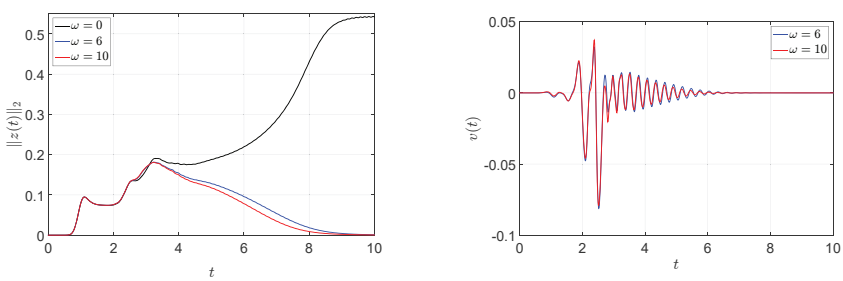

(a) L^2-norm of the controlled solutions. (b) Evolution of the controls.

FIG. 6.4. *Influence of the shift parameter ω in the stabilization results with $\beta = 45$.*

are of opposite sign. For that reason, in all the figures we have plotted only v_1.

6.1. Efficiency of control laws for $\mathbb{Z}_u = G_{\mathbb{R}}(\boldsymbol{\lambda}_1)$, $\Delta_u = \mathbf{0}_{\mathbb{R}^2}$, and $Q = \mathbf{0}_{\mathbb{R}^2}$. The corresponding feedback law is able to stabilize the Navier–Stokes equations at $R_e = 150$ for β varying from 22.5 up to 30, but not for $\beta = 45$. The stabilization results are reported in Figure 6.3.

6.2. Efficiency of control laws for $\mathbb{Z}_u = G_{\mathbb{R}}(\boldsymbol{\lambda}_1)$, $\Delta_u = \omega I_{\mathbb{R}^2}$, $\omega \geq 0$, and $Q = \mathbf{0}_{\mathbb{R}^2}$. In this section, the location of the control zone is fixed to $\theta_{\text{opt}} = 95°$, and the amplitude of the perturbation is $\beta = 45$. Let us note that for $\beta = 45$, the maximum value of $v_d \cdot n = \mu\, h_1$ in (6.2) is 0.7716, which is approximately equal to 1/2 of the maximal value 1.5 of the inflow boundary profile. The feedback is obtained by solving (6.1) with $\mathbb{Z}_u = G_{\mathbb{R}}(\boldsymbol{\lambda}_1)$, $\Delta_u = \omega I_{\mathbb{R}^2}$, $\omega \in \{0, 6, 10\}$, and $Q = \mathbf{0}_{\mathbb{R}^2}$. The evolution of the L^2-norm of the solution to the closed-loop nonlinear system is reported in Figure 6.4(a) and the corresponding controls for $\omega = 6$ and $\omega = 10$ in Figure 6.4(b).

The stabilization is achieved by choosing $\omega \in \{6, 10\}$ but not for $\omega \in \{0, 2, 4\}$. We observe that the decay rate is improved with higher values of the shift parameter ω. As expected, the norm of the control increases with the shift parameter ω. The value $\omega = 6$ seems to be a good compromise between the efficiency of a control law and a small amplitude of the control.

6.3. Comparison of different actuator locations. We compare the different actuator locations corresponding to $\theta_{\text{opt}} = 95°$, $\theta = 105°$, $\theta = 85°$, and $\theta = 75°$. The

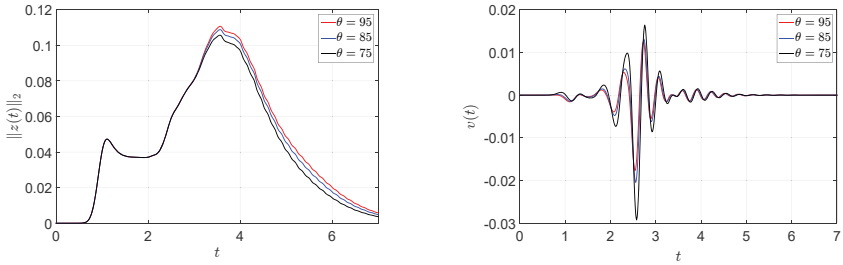

(a) L^2-norm of the controlled solutions. (b) Evolution of the controls.

FIG. 6.5. *Influence of the actuator locations on the controlled solutions* ($\omega = 0,\ \beta = 22.5$).

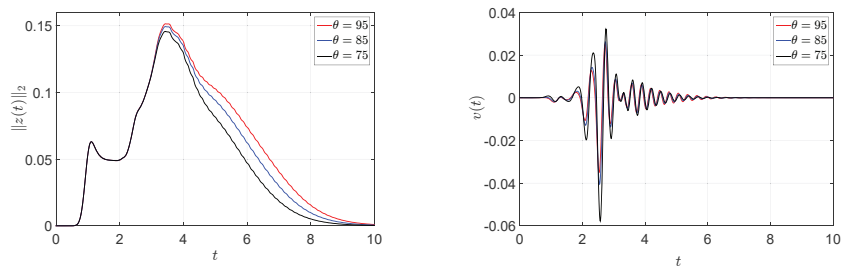

(a) L^2-norm of the controlled solutions. (b) Evolution of the controls.

FIG. 6.6. *Influence of the actuator locations on the controlled solutions* ($\omega = 0,\ \beta = 30$).

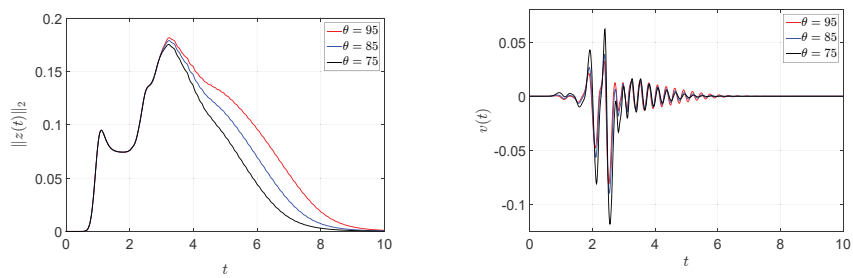

(a) L^2-norm of the controlled solutions. (b) Evolution of the controls.

FIG. 6.7. *Influence of the actuator locations on the controlled solutions* ($\omega = 6,\ \beta = 45$).

Reynolds number is still $R_e = 150$. We choose $\mathbb{Z}_u = G_{\mathbb{R}}(\boldsymbol{\lambda}_1)$, and we have tested different perturbation amplitudes $\beta = 22.5$, $\beta = 30$, and $\beta = 45$.

In Figures 6.5 and 6.6, we have reported the results for $\Delta_u = Q = \mathbf{0}_{\mathbb{R}^2}$, with $\beta = 22.5$ and $\beta = 30$, respectively, and in Figure 6.7, the results for $\Delta_u = 6\, I_{\mathbb{R}^2}$, $Q = \mathbf{0}_{\mathbb{R}^2}$, and $\beta = 45$.

If we denote by v_{105}, v_{95}, v_{85}, and v_{75} the stabilizing controls corresponding to the different actuator locations $\theta = 105°$, $\theta_{\text{opt}} = 95°$, $\theta = 85°$, and $\theta = 75°$, respectively, we can observe in Figures 6.5, 6.6, and 6.7 that the maximal amplitude of v_{95} is lower than those of v_{85} and v_{75}. For better readability, in Figures 6.5, 6.6, and 6.7 we have

TABLE 6.1
L^2-norm of the controls in terms of the control location for different perturbation amplitudes.

Control location	105°	95°	85°	75°
$\omega = 0$, $\beta = 25$	0.0120	0.0076	0.0085	0.0119
$\omega = 0$, $\beta = 30$	0.0187	0.0160	0.0180	0.0248
$\omega = 6$, $\beta = 45$	0.0416	0.0358	0.0401	0.0558

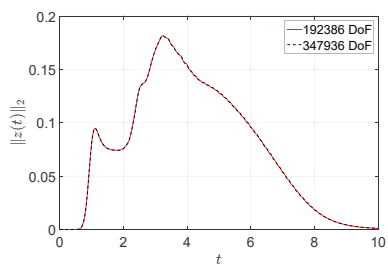

FIG. 6.8. *L^2-norm of the controlled solutions for two meshes, with $\omega = 6$ and $\beta = 45$.*

not reported the control v_{105} which is between v_{85} and v_{75}. In Table 6.1, numerical calculations show that $\|v_{95}\|_{L^2(0,\infty)}$ is smaller than $\|v_{105}\|_{L^2(0,\infty)}$, $\|v_{85}\|_{L^2(0,\infty)}$, and $\|v_{75}\|_{L^2(0,\infty)}$ in the cases corresponding to Figures 6.5, 6.6, and 6.7. This type of result is expected for the stabilization of the linearized model, but this hierarchy is still preserved for the stabilization of the Navier–Stokes system.

We note that in Figure 6.7, for $\theta = 75°$, the maximal amplitude of the control is of order 16% of the maximal amplitude of the perturbation.

Also notice that the decay in the L^2-norm of the state $z(t)$ is slightly slower for controls of smaller amplitude.

The results are stable with respect to mesh refinement. In Figure 6.8, we compare the stabilization results corresponding to the case when $\beta = 45$ and $\omega = 6$ for the current mesh (192386 degrees of freedom) and a finer one (347936 degrees of freedom).

6.4. Efficiency of control laws for $\mathbb{Z}_u = G_{\mathbb{R}}(\boldsymbol{\lambda}_1) \oplus G_{\mathbb{R}}(\boldsymbol{\lambda}_7)$. The location of the control zone is fixed at $\theta_{\text{opt}} = 95°$, and the amplitude of the perturbation at $\beta = 45$.

We compare the efficiency of feedback laws for $\mathbb{Z}_u = G_{\mathbb{R}}(\boldsymbol{\lambda}_1)$ and $\mathbb{Z}_u = G_{\mathbb{R}}(\boldsymbol{\lambda}_1) \oplus G_{\mathbb{R}}(\boldsymbol{\lambda}_7)$. We retain the eigenvalue $\boldsymbol{\lambda}_7$ because its degree of stabilizability is the greatest among the stable eigenvalues close to the imaginary axis. If we include in $\mathbb{Z}_u$ eigenvectors which are weakly controllable, the corresponding control law will provide a control of too large amplitude to be acceptable for practical applications.

We choose $\Delta_u = 6I_{\mathbb{R}^2}$ when $\mathbb{Z}_u = G_{\mathbb{R}}(\boldsymbol{\lambda}_1)$, and

$$\Delta_u = \begin{pmatrix} 6\, I_{\mathbb{R}^2} & 0 \\ 0 & 0 \end{pmatrix} \quad \text{and} \quad Q = r \begin{pmatrix} 0 & 0 \\ 0 & I_{\mathbb{R}^2} \end{pmatrix}, \quad r > 0, \tag{6.3}$$

when $\mathbb{Z}_u = G_{\mathbb{R}}(\boldsymbol{\lambda}_1) \oplus G_{\mathbb{R}}(\boldsymbol{\lambda}_7)$. In order to obtain a good compromise between a fast exponential decay of $\mathbf{z}(t)$ and a control $v(t)$ of small size, we fix $r = 3000$. The results are reported in Figure 6.9.

By choosing $\mathbb{Z}_u$ of dimension 4 and Δ_u and Q as in (6.3), the obtained exponential decay is better than in all the cases of Figure 6.7, and the maximal amplitude of the control is of order 13% of the maximal amplitude of the perturbation.

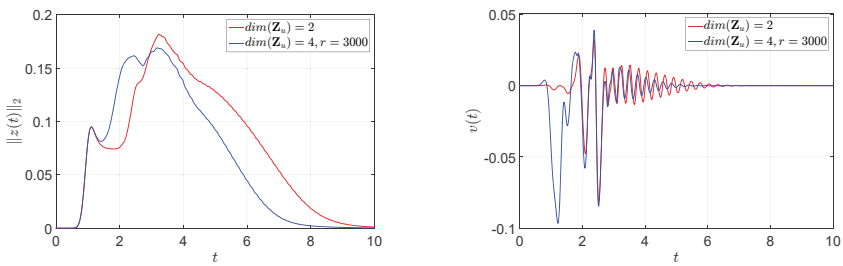

(a) L^2-norm of the controlled solutions. (b) Evolution of the controls.

FIG. 6.9. *Comparison of stabilization results with different feedback operators built with* $\dim(\mathbb{Z}_u) = 2$ *and* $\dim(\mathbb{Z}_u) = 4$.

7. Conclusion. We have determined an optimal control location by solving a min-max problem of very small dimension. This location, which corresponds to a stabilizing control of minimal norm for the linearized model, still provides a control of minimal norm for the Navier–Stokes system. The overall performance, obtained by stabilizing the projected system onto the unstable subspace, can be improved by considering the projected system onto a larger subspace (determined by analyzing the degrees of stabilizability), and by choosing a feedback control obtained via a Riccati equation involving a weighted observation operator $Q^{1/2}$, with Q of the form (6.3).

For a Reynolds number $R_e = 150$ and a perturbation of magnitude of order half of the inflow boundary condition, localized in time around $t = 1$, we first notice the development of a vortex shedding which is totally cancelled at $t = 8$ or $t = 9$ depending on the control law. The maximal amplitude of the control is of order 13% of the maximal amplitude of the perturbation when the vortex shedding is cancelled at $t = 8$ and of order 6% when the vortex shedding is cancelled at $t = 9$. Being able to control the rate between the maximal amplitude of the control and the maximal amplitude of the perturbation might be important for practical applications.

8. Appendix.

Nonhomogeneous Dirichlet condition in strong form. Let us explain what the semidiscrete controlled system is if the boundary condition $z = v_c$ on Σ_d^∞ is imposed in a strong sense. For that, we set

$$z = \sum_{i=1}^{N_y} z_i \phi_i + \sum_{k=1}^{N_b} \sum_{j=1}^{N_c} v_j(t) g_k^j \phi_k.$$

The indices $1 \leq i \leq N_y$ correspond to the degrees of freedom of the interior nodes, while the indices $1 \leq k \leq N_b$ correspond to the degrees of freedom of the boundary nodes where nonhomogeneous Dirichlet boundary conditions are imposed. We set $\mathbf{z} = (z_1, \cdots, z_{N_y})^T \in \mathbb{R}^{N_y}$. We introduce the mass matrices M_{yy}, $M_{yb} = M_{by}^T$, and M_{bb}, the coefficients of which are defined by

$$M_{yy}^{ij} = (\phi_i, \phi_j), \quad M_{yb}^{ik} = (\phi_i, \phi_k), \quad M_{bb}^{k\ell} = (\phi_k, \phi_\ell)$$

for $1 \le i,\, j \le N_y$, $1 \le k,\, \ell \le N_b$. The other matrices A_{yy}, A_{yb}, A_{yp}, B_{yp}, and $\mathbf{G}$, involved in the semidiscrete system, are defined by

$$\begin{aligned}
&A_{yy}^{ij} = a(\phi_j, \phi_i), \quad A_{yb}^{ik} = a(\phi_k, \phi_i) \quad \text{for } 1 \le i,\, j \le N_y,\ 1 \le k \le N_b,\\
&A_{yp}^{ij} = b(\phi_i, \psi_j) \quad \text{for } 1 \le i \le N_y,\ 1 \le j \le N_p,\\
&B_{yp}^{ik} = b(\phi_k, \psi_i) \quad \text{for } 1 \le i \le N_p,\ 1 \le k \le N_b,\\
&\mathbf{G}^{kj} = g_k^j \quad \text{for } 1 \le k \le N_b,\ 1 \le j \le N_y.
\end{aligned}$$

We assume that A_{yp} is of rank $N_p < N_y$. The projector $\mathbb{\Pi}_y^T$ onto $\mathrm{Ker}(A_{yp}^T)$ parallel to $\mathrm{Im}(M_{yy}^{-1} A_{yp})$ is

$$\mathbb{\Pi}_y^T = I_{\mathbb{R}^{N_y}} - M_{yy}^{-1} A_{yp} (A_{yp}^T\, M_{yy}^{-1}\, A_{yp})^{-1} A_{yp}^T. \tag{8.1}$$

The semidiscrete system is now

$$\begin{aligned}
&M_{yy}\mathbf{z}'(t) + M_{yb}\mathbf{G}\mathbf{v}'(t) = A_{yy}\mathbf{z}(t) + A_{yb}\mathbf{G}\mathbf{v}(t) + A_{yp}\mathbf{p}(t),\\
&A_{yp}^T\mathbf{z}(t) + B_{yb}\mathbf{G}\mathbf{v}(t) = 0.
\end{aligned} \tag{8.2}$$

If $\mathbf{v} \in H^1(0,\infty;\mathbb{R}^{N_c})$, as in section 3.2, we can prove that the pair $(\mathbf{z}, \mathbf{p})$ is a solution to (8.2) if and only if it is a solution to

$$\begin{aligned}
&\mathbb{\Pi}_y^T(\mathbf{z} + M_{yy}^{-1} M_{yb} G\mathbf{v})'(t) = \mathbf{A}\mathbb{\Pi}_y^T(\mathbf{z} + M_{yy}^{-1} M_{yb} G\mathbf{v})(t) + \mathbf{B}\mathbf{v}(t),\\
&(I - \mathbb{\Pi}_y^T)(\mathbf{z} + M_{yy}^{-1} M_{yb} G\mathbf{v})(t)\\
&\qquad = -M_{yy}^{-1} A_{yp} (A_{yp}^T\, M_{yy}^{-1}\, A_{yp})^{-1} A_{yp}^T (B_{yb} - M_{yy}^{-1} M_{yb})\mathbf{G}\,\mathbf{v}(t),
\end{aligned} \tag{8.3}$$

with

$$\begin{aligned}
\mathbf{p}(t) &= (A_{yp}^T\, M_{yy}^{-1}\, A_{yp})^{-1} A_{yp}^T M_{yy}^{-1} \Big(M_{yy}\mathbf{z}'(t) + M_{yb} G\mathbf{v}'(t) - A_{yy}\mathbf{z}(t) - A_{yb}\mathbf{G}\mathbf{v}(t) \Big),\\
\mathbf{A} &= \mathbb{\Pi}_y^T M_{yy}^{-1} A_{yy}, \text{ and}\\
\mathbf{B} &= -\mathbb{\Pi}_y^T M_{yy}^{-1} \Big(A_{yy} M_{yy}^{-1} A_{yp} (A_{yp}^T\, M_{yy}^{-1}\, A_{yp})^{-1} B_{yb} + A_{yy} \mathbb{\Pi}_y^T M_{yy}^{-1} M_{yb} - A_{yb} \Big)\mathbf{G}.
\end{aligned}$$

The consistent initial condition for system (8.3) is

$$\mathbb{\Pi}_y^T(\mathbf{z} + M_{yy}^{-1} M_{yb} G\mathbf{v})(0) = \mathbb{\Pi}_y^T(\mathbf{z}_0 + M_{yy}^{-1} M_{yb} G\mathbf{v}(0)), \tag{8.4}$$

and the consistent initial condition for system (8.2) is

$$\begin{aligned}
(\mathbf{z} + M_{yy}^{-1} M_{yb} G\mathbf{v})(0) &= \mathbb{\Pi}_y^T(\mathbf{z}_0 + M_{yy}^{-1} M_{yb} G\mathbf{v}(0))\\
&\quad - M_{yy}^{-1} A_{yp} (A_{yp}^T\, M_{yy}^{-1}\, A_{yp})^{-1} A_{yp}^T \Big(B_{yb} + M_{yy}^{-1} M_{yb} \Big)\mathbf{G}\mathbf{v}(0).
\end{aligned} \tag{8.5}$$

Thus, we have the following result.

THEOREM 8.1. *Assume that* $\mathbf{v}$ *belong to* $H^1(0,\infty;\mathbb{R}^{N_c})$. *A pair* $(\mathbf{z}, \mathbf{p})$ *is a solution of* (8.2) *with the initial condition* (8.5) *if and only if* $(\mathbf{z}, \mathbf{p})$ *is the solution to system* (8.3) *with the initial condition* (8.4).

Comparison with the controlled system obtained in [19]. In [19], the matrix M_{yb} is taken equal to $\mathbf{0}_{N_y \times N_b}$. In that case, (8.3) and (8.2) correspond to equation (6.6a) in [19]. This is justified if a mass lumping method is used; see, e.g., [12]. This type of simplification can be used for stable systems (as in [19]) or for moderately unstable systems. But it is not accurate enough for the stabilization of unstable systems.

REFERENCES

[1] E. Åkervik, J. Hœpffner, U. Ehrenstein, and D.S. Henningson, *Optimal growth, model reduction and control in a separated boundary-layer flow using global eigenmodes*, J. Fluid Mech., 579 (2007), pp. 305–314.

[2] L. Amodei and J.-M. Buchot, *A stabilization algorithm of the Navier-Stokes equations based on algebraic Bernoulli equation*, Numer. Linear Algebra Appl., 19 (2012), pp. 700–727.

[3] M. Badra, *Stabilisation par Feedback et Approximation des Equations de Navier-Stokes*, Ph.D. thesis, Université Paul Sabatier Toulouse III, Toulouse, France, 2006; available online at http://mbadra.perso.univ-pau.fr/THESE-BADRA.pdf.

[4] M. Badra and T. Takahashi, *Stabilization of parabolic nonlinear systems with finite dimensional feedback or dynamical controllers: Application to the Navier–Stokes system*, SIAM J. Control Optim., 49 (2011), pp. 420–463, https://doi.org/10.1137/090778146.

[5] E. Bänsch, P. Benner, J. Saak, and H.K. Weichelt, *Riccati-based boundary feedback stabilization of incompressible Navier–Stokes flows*, SIAM J. Sci. Comput., 37 (2015), pp. A832–A858, https://doi.org/10.1137/140980016.

[6] A. Barbagallo, D. Sipp, and P.J. Schmid, *Closed-loop control of an open cavity flow using reduced-order models*, J. Fluid Mech., 641 (2009), pp. 1–50.

[7] D. Barkley, *Linear analysis of the cylinder wake mean flow*, Europhys. Lett., 75 (2006), pp. 750–756.

[8] P. Benner and J. Heiland, *Time-dependent Dirichlet conditions in finite element discretizations*, ScienceOpen Research, (2015), https://doi.org/10.14293/S2199-1006.1.SOR-MATH.AV2JW3.v1.

[9] P. Benner, J. Saak, M. Stoll, and H.K. Weichelt, *Efficient solution of large-scale saddle point systems arising in Riccati-based boundary feedback stabilization of incompressible Stokes flow*, SIAM J. Sci. Comput., 35 (2013), pp. S150–S170, https://doi.org/10.1137/120881312.

[10] M. Bergmann and L. Cordier, *Optimal control of the cylinder wake in the laminar regime by trust-region methods and POD reduced-order models*, J. Comput. Phys., 227 (2008), pp. 7813–7840.

[11] D. Boffi, *Finite element approximation of eigenvalue problems*, Acta Numer., 19 (2010), pp. 1–120.

[12] J.-M. Buchot, J.-P. Raymond, and J. Tiago, *Coupling estimation and control for a two dimensional Burgers type equation*, ESAIM Control Optim. Calc. Var., 21 (2015), pp. 535–560.

[13] K.K. Chen and C.W. Rowley, *$H2$ optimal actuator and sensor placement in the linearised complex Ginzburg-Landau system*, J. Fluid Mech., 681 (2011), pp. 241–260.

[14] H. Choi, W.-P. Jeon, and J. Kim, *Control of flow over a bluff body*, in Annu. Rev. Fluid Mech. 40, Annual Reviews, Palo Alto, CA, 2008, pp. 113–139.

[15] COMSOL Multiphysics Version 5.3, COMSOL, 2017.

[16] A.V. Fursikov and R. Rannacher, *Optimal Neumann control for the two-dimensional steady-state Navier-Stokes equations*, in New Directions in Mathematical Fluid Mechanics, Adv. Math. Fluid Mech., Birkhäuser Verlag, Basel, 2010, pp. 193–221.

[17] M.D. Gunzburger and S.L. Hou, *Treating inhomogeneous essential boundary conditions in finite element methods and the calculation of boundary stresses*, SIAM J. Numer. Anal., 29 (1992), pp. 390–424, https://doi.org/10.1137/0729024.

[18] J.-W. He, M. Chevalier, R. Glowinski, R. Metcalfe, A. Nordlander, and J. Periaux, *Drag reduction by active control for flow past cylinders*, in Computational Mathematics Driven by Industrial Problems, Springer, Berlin, 2000, pp. 287–363.

[19] M. Heinkenschloss, D.C. Sorensen, and K. Sun, *Balanced truncation model reduction for a class of descriptor systems with application to the Oseen equations*, SIAM J. Sci. Comput., 30 (2008), pp. 1038–1063, https://doi.org/10.1137/070681910.

[20] K. Hiramoto, H. Doki, and G. Obinata, *Optimal sensor/actuator placement for active vi-*

bration control using explicit solution of algebraic Riccati equation, J. Sound Vibration, 229 (2000), pp. 1057–1075.

[21] S. Kesavan and J.-P. Raymond, *On a degenerate Riccati equation*, Control Cybernet., 38 (2009), pp. 1393–1410.

[22] R.B. Lehoucq, D.C. Sorensen, and C. Yang, *ARPACK Users' Guide: Solution of Large-Scale Eigenvalue Problems with Implicitly Restarted Arnoldi Methods*, SIAM, Philadelphia, 1998, https://doi.org/10.1137/1.9780898719628.

[23] V. Maz'ya and J. Rossmann, *Mixed boundary value problems for the stationary Navier-Stokes system in polyhedral domains*, Arch. Ration. Mech. Anal., 194 (2009), pp. 669–712.

[24] K. Morris, *Linear-quadratic optimal actuator location*, IEEE Trans. Automat. Control, 56 (2011), pp. 113–124.

[25] K. Morris and M.A. Demetriou, *Using H_2-control performance metrics for the optimal actuator location of distributed parameter systems*, IEEE Trans. Automat. Control, 60 (2015), pp. 450–462.

[26] P.A. Nguyen and J.-P. Raymond, *Boundary stabilization of the Navier–Stokes equations in the case of mixed boundary conditions*, SIAM J. Control Optim., 53 (2015), pp. 3006–3039, https://doi.org/10.1137/13091364X.

[27] D.S. Park, D.M. Ladd, and E.W. Hendricks, *Feedback control of Von Karman vortex shedding behind a circular cylinder at low Reynolds numbers*, Phys. Fluids, 6 (1994), pp. 2390–2405.

[28] J. Pitkäranta, *Boundary subspaces for the finite element method with Lagrange multipliers*, Numer. Math., 33 (1979), pp. 273–289.

[29] J.-P. Raymond, *Feedback boundary stabilization of the two-dimensional Navier–Stokes equations*, SIAM J. Control Optim., 45 (2006), pp. 790–828, https://doi.org/10.1137/050628726.

[30] J.-P. Raymond, *Feedback boundary stabilization of the three-dimensional incompressible Navier-Stokes equations*, J. Math. Pures Appl. (9), 87 (2007), pp. 627–669.

[31] J.-P. Raymond and L. Thevenet, *Boundary feedback stabilization of the two dimensional Navier-Stokes equations with finite dimensional controllers*, Discrete Contin. Dyn. Syst., 27 (2010), pp. 1159–1187.

[32] Y. Renard and J. Pommier, *GetFEM++. An Open Source Finite Element Library*, 2017, http://getfem.org.

[33] R. Stenberg, *Error analysis of some finite element methods for the Stokes problem*, Math. Comp., 54 (1990), pp. 495–508.

[34] M. van de Wal and B. de Jager, *A review of methods for input/output selection*, Automatica J. IFAC, 37 (2001), pp. 487–510.